UTILIZING GROUND LEVEL REMOTE SENSING TO MONITOR PEATLAND DISTURBANCE

By: Cameron N. McCann, B.Sc.

Submitted to the School of Graduate Studies in Partial Fulfillment of the Requirements for the Degree Master of Science

MASTER OF SCIENCE (2016) MCMASTER UNIVERSITY
(EARTH AND ENVIRONMENTAL SCIENCE) HAMILTON, ONTARIO

TITLE: Utilizing Ground Level Remote Sensing to Monitor Peatland Disturbance

AUTHOR: Cameron N. McCann, B.Sc. (McMaster University)

SUPERVISOR: Dr. James M. Waddington

NUMBER OF PAGES: viii, 92

ABSTRACT

This study examined the usefulness of remote sensing to monitor peatlands, and more specifically *Sphagnum* moss 'health'. Results from this study show that thermal imaging can be used to monitor *Sphagnum* productivity, as when the surface temperature of *Sphagnum* exceeds a threshold value (30.8 °C in the field and 18.2 °C in the laboratory), *Sphagnum* quickly changes from being productive to being unproductive. The Enhanced Normalized Difference Vegetation Index (ENDVI) can also be used in a similar manner, where if the ENDVI value is high (above 0.11 in the field and -0.12 in the laboratory), *Sphagnum* will be productive, and otherwise, it will be stressed.

A classification scheme was developed to monitor peatland recovery to fire disturbance. By utilizing the ENDVI, leaf area index and aboveground biomass within a recovering peatland can be mapped, as well as the recovery trajectory of the groundcover. The findings of this study highlight the potential use of remote sensing to assess the driving factors of *Sphagnum* moss stress, as well as quickly and expansively aid in peatland recovery trajectory.

ACKNOWLEDGEMENTS

I would first like to thank my supervisor, Dr. Mike Waddington for this amazing opportunity, but for all the support he has given me over the last few years. I am so grateful for all the input and enthusiasm that he has shown towards this project. I know it was a learning experience for both of us, and the level of trust he shows towards me was a huge confidence booster. I am looking forward to staying apart of such an amazing group that he has put together.

To all the people within the McMaster Ecohydrology Group; all the help throughout the past 2 years is greatly appreciated. I'm so happy to have worked with each and every one of you. Thank-you to Sophie Wilkinson for all of her invaluable input and advice. Thanks to Alanna Smolarz, Kristyn Housman, and Rebekah Ingram for all the help in the field, and as well to Ben Didemus. I don't think I will ever again hike as much in my life as I have with Ben.

Thank-you to all the members of the McMaster Watershed Hydrology Group for welcoming me into their office, and a special thanks to Victor Tang for all his help with MATLAB.

And finally, a big thanks to my family and friends for all their support over the past few years.

TABLE OF CONTENTS

LIST OF FIGURES

LIST OF TABLES

CHAPTER 1: INTRODUCTION

Subarctic and boreal peatlands have stored approximately 455 Pg of carbon during the Holocene (Gorham, 1991). Approximately 56% of all organic soil carbon in Canada (147 Pg of carbon) is currently stored in peatlands (Tarnocai, 2006). However, there is concern that long-term carbon sink function of these peatlands is vulnerable to drought (Kettridge and Waddington, 2014) and wildfire disturbance (Turetsky *et al.*, 2002). These disturbances can effectively change this long-term storage function of a peatland by reducing moss productivity, and increasing the rate of decomposition (Freeman *et al.*, 1993; Kettridge and Waddington, 2014) and combustion (Turetsky *et al.*, 2002). *Sphagnum* peat moss is estimated to have the most carbon storage, dead or alive, in comparison to any other genus of plant (Clymo and Hayward, 1982; van Breeman, 1995). Despite this important aspect of Canada's carbon budget, very little research has been conducted on efficiently monitoring the 'health' of moss or a peatland using remote sensing, which is a useful tool that has previously been applied to land-use change, forestry, and agricultural monitoring (Jones and Vaughn, 2010).

In general, the varying microtopography and water table (WT) proximity are the main factors affecting species distribution within and among peatlands (Vitt, 1990). These two environmental factors create various ranges of microhabitats, where different species have a competitive advantage within certain environmental niches (Benscoter and Vitt, 2008). *Sphagnum* mosses in general

are able to effectively draw water up from the WT to stay moist, although some species are more efficient at it than others. These species of moss rely entirely upon passive capillary action to transport this water to the capitula; the live, growing section of moss. Due to this process, *Sphagnum* production rates can be limited by soil moisture, which in turn, limits the carbon sequestration potential (Thompson and Waddington, 2008). Moisture content and WT position are also the major factors affecting peatland-atmosphere carbon dioxide and methane exchange which determines the net carbon flux of the ecosystem (Dise *et al.*, 1993; Harris *et al.*, 2005). The net gain of carbon by peatland ecosystems is predominantly stored below ground as the extremely recalcitrant nature of peat moss makes it hard to break down (Gerdol and Vicentini, 2011).

1.1 *SPHAGNUM* BOGS

Sphagnum, like most other moss, grows at its apex. This apex produces branches, and while these branches grow and elongate, the internodes of the main stem do not. This results in the formation of the capitula, a compact hemispherical head, which is the main living portion of the *Sphagnum* moss (Clymo and Hayward, 1982). As the *Sphagnum* moss grows vertically, the growth of new branches abovie will shade and kill lower branches (typically within a year or two). The only portion that can survive under the moss is any axillary buds (Clymo and Hayward, 1982), which typically remain inactive unless the capitula (or apex) is

destroyed. As the branches die, the extremely recalcitrant nature of *Sphagnum* peat moss (Gerdol and Vincentini, 2011) makes it difficult for them to degrade biologically (Providenti *et al.*, 1993).

Accumulated peat can persist long after the death of the moss, lasting hundreds to thousands of years (Jones *et al.*, 1994). As it deposits it creates bogs, which are areas where waterlogged peat can build up to levels above the surrounding water system (Ingram, 1982). The growth of *Sphagnum* positively feedbacks on its own growth and autogenically changes the supply of resources, turning it into a habitat where few other plants can survive (van Breeman, 1995, Rochefort 2000). Some *Sphagnum* species can create microtopographic features with these bogs that are raised (hummocks) in relation to other lower lying areas (hollows) (Johnson *et al.*, 2015). At low water contents, different *Sphagnum* species have been shown to have different photosynthetic abilities (Titus *et al.*, 1983; Gerdol *et al.*, 1996). For example, *Sphagnum fuscum* (a hummock species) when compared to *Sphagnum magellanicum* and *Sphagnum fallax* (hollow species) has been shown to be almost insensitive to the water level (Grosvernier *et al.*, 1997), meaning it maintains productivity even when the WT drops. When there is a hydrological disconnection, the near-surface will have increased tension (Clymo and Hayward, 1982), limiting water loss from the surface (Kettridge and Waddington, 2014), which will maintain moist conditions through most of the peat's profile. This, however, causes an increase in peat surface temperature, with the near-surface acting as an insulator and keeping the subsurface cool (Kettridge *et al.*, 2012).

When the surface is wet, if the evaporative demand increases, evaporation will lower the temperature of the peat surface below the air temperature. However, when the surface resistance to evaporation increases, the surface temperature will also increase due to the latent heat flux being reduced (Kettridge and Waddington, 2014). Such changes in temperature can likely be monitored using remote sensing.

When the WT is within 0.3 m of the peat surface, water moving through the vadose zone is not equal to that lost by evaporation, and therefore water is lost from storage in the near surface. This produces high tensions, which are in hydrostatic disequilibrium from the WT (Kettridge and Waddington, 2014). If the WT drops lower than a threshold value, the ability of moss to conduct water through capillary rise will become restricted, lowering the rate of water supply from the saturated zone, which in turn will restrict evaporative loss (Waddington *et al.*, 2015). Williams and Flanagan (1996) have shown that photosynthetic gas exchange by moss is limited by low water content in a black spruce (*Picea mariana)* forest, due to an overall decrease in metabolic processes. Conversely, at a water content above an optimum level, *Sphagnum* can also become less productive (Tuittila *et al.*, 2004). Murray *et al.* (1993) showed that in shaded plots, which had less evaporative loss, moss growth was 2-3 times higher in comparison to the control plots, while plots that had their canopies removed (no longer shaded) had a large reduction in moss productivity. *Sphagnum capilifolium* (a hummock species) has been shown to have a slower evaporation

rate, allowing for better water retention, and causing photosynthesis to shut down later as a result (Gerdol *et al.*, 1996). The decrease in photosynthetic capacity was correlated with a decrease in the quantum yield of photosystem II (F_v/F_m) in mosses (Murray *et al.*, 1993).

In an undisturbed ecosystem, once there has been an establishment of a partial moss carpet from true mosses; water retention increases, and there are fewer issues with substrate instability (Rochefort, 2000). This moss carpet will expand at rates that depend upon the slope gradient of the underlying material or terrain (Bauer *et al.*, 2003). *Sphagnum* relies on passive water transport, making them very susceptible to soil moisture variation. Approximately 80 - 90% of *Sphagnum* water content is held between its branches and leaves (Clymo and Hayward, 1982; Bubier *et al.*, 1997) with the other 10 - 20% used by its chloroplasts for photosynthesis (Proctor and Smirnoff, 2000; Thompson and Waddington, 2008). *Sphagnum's* hyaline cells absorb water rapidly, but when emptied during drought *Sphagnum* will turn white, causing the albedo of the moss to rise (van Breeman, 1995). This white appearance, known as *Sphagnum* bleaching (Harris *et al.*, 2005), has a negative effect outlined by Waddington *et al.*, 2015, as part of the Water Table Depth-Moss Surface Resistance and Albedo Feedback. These changes in colour can also be monitored using remote sensing.

Sphagnum is not only affected by its water content, but by available light. At low levels of photosynthetically active radiation (PAR), vascular plants are unable to

photosynthesize. At high light levels, *Sphagnum* moss will also exhibit a lower photosynthetic capacity. This photoinhibition can lead to lowered carbon exchange, affecting the CO_2 flux at the ecosystem level (Murray *et al.*, 1993). Typically, at higher light levels, the temperature will also be higher. Gerdol and Vicentini (2011) showed that high temperatures cause a decrease in nitrogen and chlorophyll concentrations, leading to a lower quantum yield of photosystem II and net CO_2 exchange rates. The same response occurred in both *S. magellanicum* and *S. fuscum*.

1.2 FIRE AND *SPHAGNUM*

Wildfire is one of the most predominant peatland disturbances within the Western Boreal Plains (Turetsky, 2002). It has been shown that the variability in charcoal deposition and removal of ground level vegetation by fire results in a range of starting points for post-fire re-vegetation (Benscoter, 2006). This variability in vegetation removal is due to the peatland properties [spatial variability in species composition and hydrology within the site (Benscoter and Wieder, 2003)] before a fire, and the intensity of the fire (Lukenbach *et al.*, 2015b). Hummock species, such as *S. fuscum* are more densely packed together, and as such have better water retention than hollow species, such as *Sphagnum angustifolium*, under the same conditions (Benscoter and Vitt, 2008). As such, more energy is required to drive off moisture for ignition in *S. fuscum* hummocks, thereby reducing its burn

severity in comparison to hollow species (Shetler *et al.*, 2008; Kettridge *et al.*, 2012). Benscoter and Wieder (2003) showed that hollows that experience a higher burn severity exhibit greater organic matter loss. They found that almost twice as much carbon was released from hollows (2.76 kg C m^{-2}) in comparison to hummocks (1.45 kg C m^{-2}).

Although peatland wildfire will typically result in the die-off of ground layer vegetation and complete stand mortality (Zoltai et al., 1998; Benscoter and Vitt, 2008), peatlands are generally resilient to wildfire as they will return to a net carbon sink within 20 years of burning (Wieder et al., 2009). In the first 10 years post-fire, the largest amount of community change occurs within the ground layer vegetation (Benscoter and Vitt, 2008). Benscoter (2006) found that post-fire *Sphagnum* mosses rarely occurred in the absence of true mosses and *Sphagnum* was only present in one-third of the plots that had true moss colinization. The greater occurrence of *Sphagnum* mosses alongside true moss suggests that post-fire microhabitat modification may be required for the successful establishment of *Sphagnum* (Benscoter, 2006). Once Sphagnum has re-established, the rate of expansion of these nucleation sites is predominantly dependent on moisture availability and topography (Bauer *et al.*, 2003).

Ericaceous plants, such as *Rhodedendron groenlandicum*, become more abundant after the passage of a low-severity fire (Foster, 1985; Nguyen-Xuan *et al.*, 2000) as their deep reproductive organs (Flinn and Wein, 1977) are typically unaffected

(Lecomte *et al.*, 2005). However, when deep burning occurs, few ericaceous shrubs will return immediately after fire (Lecomte *et al.*, 2005; 2006). These ericaceous species have a detrimental effect on *Picea mariana* recolonization and growth due to water-soluble phenolics and their ability to influence ecosystem processes such as nutrient cycling (Nilsson *et al.*, 1993; Mallik and Mallik, 1997; Lecomte *et al.*, 2005).

1.3 CHLOROPHYLL-FLUORESCENCE

Recovery, growth, or stress of an ecosystem is typically estimated based on the level of photosynthetic activity. Chlorophyll-Fluorescence (Chl-F) has become a simple yet useful approach, both in the laboratory and the field, to obtain information on photosynthesis (van Kooten and Snel, 1990). Fluorescence measurements can be made using a variety of methods, but generally include some form of dark adaption before pulsing the plant sample with high intensity light of around 675nm (Chapelle *et al.*, 1992) and measuring the sample's emission of this wavelength before and after. The potential quantum yield of photosystem II (PSII) is one of the most widely used quantitative measurements for Chl-F and can be measured using the ratio of variable maximal fluorescence, F_v/F_m (Bilger et al., 1995). In this equation; F_v is the maximum variable fluorescence when non-photochemical processes are at a minimum (F_m-F_o); F_m is the fluorescence intensity when all PSII reaction centers are closed and non-

photochemical quenching is at a minimum; and F_o is the intensity when all PSII reaction centers are open while the photosynthetic membrane is in the non-energized state (van Kooten and Snel, 1990). This equation; as well as F_v/F_o (a value proportionate to the water-splitting complex on the donor side of the PSII) (Kalaji *et al.*, 2011), have been used to monitor the Chl-F signature of the photosynthetic apparatus in relation to acute stress (Demmig and Björkman, 1987; Bilger *et al.*, 1995; Lichtenthaler and Miehé, 1997). Fluorescence imagery, although allowing for early detection of stress, is unable to identify the specific stress that is imposed (Lichtenthaler and Miehé, 1997; Chaerle and Van Der Straeten, 2000), which can limit its applicability.

In the field, miniaturized pulse-amplitude modulated photosynthesis yield analyzers have been used to monitor photosynthesis and stress at the leaf level. However, as photosynthesis may not be in steady state in the field, this method can be criticized (Rascher *et al.*, 2000). When conducting fluorescence measurements in the field, it is important to dark-adapt a sample for 20-30 minutes to accurately measure the acute photoinhibition shown by F_v/F_m (Thiele and Krause, 1994; Rascher *et al.*, 2000). Zarco-Tejada *et al.* (2002) used a series of laboratory measurements of spectral reflectances to show that remote sensing can be used to accurately detect the effects of Chl-F. The use of these remote sensing techniques could help identify larger temporal and spatial scales of stress before damage is even visible as changes in chlorophyll function often precede changes in chlorophyll content (when a leaf becomes chloritic) (Zarco-Tejada *et*

al., 2002). Many methods of monitoring fluorescence using remote sensing have become more prevalent, the most common being the use of fluorescence ratios, the red-edge and vegetation indices. Thermal imaging has also been used to monitor plant stress (Chaerle and Van Der Straeten, 2000).

The major part of light, which is absorbed by photosynthetic pigments, chlorophyll, and carotenoids, is used for the photosynthetic quantum conversion (Lichtenthaler and Babani, 2000). However, under normal physiological conditions, only a small portion is de-excited through emission as heat or as red and far-red fluorescence. Using these fluorescence emissions, the fluorescence ratios blue : red and blue : far-red can be calculated, which are particularly sensitive to environmental stress (Lichtenthaler and Miehé, 1997).

1.4 VEGETATION INDICES

For broader approaches to measuring photosynthesis and stress, spectral or vegetation indices that utilize the spectral features or properties of plant leaves are used to measure the chlorophyll concentration and activity of a plant (Gitelson and Merzlyak, 1998). Thermal, reflectance and fluorescence imaging have shown that changes in light emission from leaves can be used as an indication of the level of stress (Chaerle and Van Der Straeten, 2000). Spectral indices are mathematical combinations of multiple spectral bands that are designed to relate to biophysical parameters such as Leaf Area Index (LAI) and water content. The idea of

utilizing the measurements of multiple wavelengths has been widely adopted within remote sensing, especially for studying vegetation cover through the use of these vegetation indices (Jones and Vaughn, 2010). Vegetation indices are generally dimensionless equations used as surrogates to indicate the presence, cover, and health of green vegetation (Jones and Vaughn, 2010).

Stressed leaves or vegetation have less absorption (more reflection) by pigments in the visible spectrum (Carter, 1993). It has been shown that linear combinations between the red and near infrared bands are sensitive to green leaf area and biomass. The red band exhibits a nonlinear relationship between integrated spectral radiance and green biomass, while the near infrared band has a direct linear relationship (Tucker, 1979). Since these relationships are caused by a plant's physiology (i.e. healthy or stressed), they can be measured using remote sensing and be combined to create vegetation index representations.

The Normalized Difference Vegetation Index (NDVI), $(\rho_{NIR}-\rho_R)/(\rho_{NIR}+\rho_R)$, where ρ represents the reflectance in one of the broadband channels, is one of the most widely used vegetation indices. The NDVI tends to be sensitive to low chlorophyll concentrations, the fraction of vegetation cover, and as a result, the absorbed PAR (Yoder and Waring, 1994). The NDVI is the most widely used vegetation index when estimating LAI (Steltzer and Welker, 2006; Jones and Vaughn, 2010). Gitelson *et al.* (1996) found that the chlorophyll-a concentration was proportional to the inverse of the green band's reflectance, thus they replaced

the red band with the green band in the NDVI to create the Green Normalized Difference Vegetation Index (GNDVI), $(\rho_{NIR}-\rho_G)/(\rho_{NIR}+\rho_G)$; (Gitelson and Merzlyak, 1998). Furthermore, Wang et al. (2007) found that by using both green and blue band reflectances to replace the red band and create a Green-Blue NDVI (GBNDVI), $(\rho_{NIR}-(\rho_G+\rho_B))/(\rho_{NIR}+(\rho_G+\rho_B))$, a better estimation of LAI could be made. The ratio images created by using these equations, when expressed in false colour, allow for quick detection of declining photosynthetic activity (Lichtenthaler and Babani, 2000).

Although these and many other vegetation indices have successfully been used in the estimation of biomass, LAI, leaf stress, and overall plant health (Huete *et al.*, 1997; Steltzer and Welker, 2006; Jones and Vaughn, 2010; Hunt *et al.*, 2013); they are all designed with the idea that the plant species are going to be green in colour (caused by chlorophyll content). For most plant communities, these are very appropriate, but for ecosystems that are dominated by plants of various colours, this approach may not be ideal. Peatlands that have a ground cover that is dominated by moss (such as *Sphagnum* or feathermoss) will have very different spectral signatures, however, it has been shown that *Sphagnum* photosynthetic activity, and relative changes in moss water content can be monitored using measurements of spectral reflectance (Van Gaalen *et al.*, 2007). The spectral signature of the ecosystem will depend on the amount of overstory vegetation as the moss may be the dominant species, having the most influence on the peatlands

signal, or it may just be part of the background, having little to no effect (Vogelmann and Moss, 1993).

The near-infrared reflectance of moss is typically lower than vascular plants and is generally characterized by strong water absorption features (Bubier *et al.*, 1997). Even within the genus of *Sphagnum*, each individual species can exhibit different reflectance properties. Some species, which are green in colour (*S. fallax*, *S. cuspidatum*), have reflectance peaks around 0.55 μm, which is related to their chlorophyll content. Other species, such as *S. capillifolium* and *S. warnstorfii* have a prominent peak in reflectance at 0.63 μm, which is related to the presence and abundance of sphagnorubin (a reddish biochemical pigment associated with some *Sphagnum* species cell walls) (Gorham, 1990; Vogelmann and Moss, 1993). There are also *Sphagnum* species that tend to be a yellow-brown colour (*S. papillosum*, *S. fuscum*) which have peaks related to both their chlorophyll content in the green band, and sphagnorubin in the red band (Vogelmann and Moss, 1993).

1.5 CHANGE DETECTION

By using datasets acquired at two different times, change detection techniques can be applied to monitor differences in biophysical environments over time (Singh, 1989; Miller and Yool, 2002; Lu *et al.*, 2004; Lunetta *et al.*, 2006). The NDVI data collected from Moderate-Resolution Imaging Spectroradiometer (MODIS)

has been shown to be a quick and easy change detection approach in monitoring land-cover change (Lunetta *et al.*, 2006). Gouveia *et al.* (2012) found that it is useful to evaluate intra-annual changes in the NDVI (δNDVI) as an indication of the greenness of vegetation as a means of monitoring drought severity through the change in photosynthetic activity (estimated from the NDVI).

After the passage of a fire, information linking the spatiotemporal variability and vegetation impacts is necessary to not only quantify the fire impact, but to monitor recovery and restoration (Gitas *et al.*, 2009). By applying change detection techniques, and more specifically, using the subtraction of images, the response of vegetation to fire can be easily monitored using variations in vegetation indices or colour composites (Diaz-Delgado and Pons, 2001). By utilizing the increase in reflectance of the NIR band with the re-establishment of vegetation cover, vegetation indices, such as the NDVI, can be used as a surrogate to monitor the chronosequence of vegetation recovery (Epting and Verbyla, 2005).

1.6 THESIS OBJECTIVES

There are two primary objectives to this study. The first is to identify the remote sensing techniques that can be applied to monitor the 'health' status of peatland moss, more specifically the genus *Sphagnum*. The second primary objective is to

identify the remote sensing techniques that can be used to monitor recovery of a peatland from fire disturbance.

CHAPTER 2: UTILIZING REMOTE SENSING TO MONITOR *SPHAGNUM* 'HEALTH' AND PRODUCTIVITY

2.1 INTRODUCTION

In Canada, peatlands cover approximately 1.14 million km^2, accounting for ~56% of all organic carbon (C) stored in Canadian soils. These Canadian peat deposits store an estimated 147 Pg C (Tarnocai, 2006). Globally, these ecosystems contain approximately one-third of all soil carbon (Gorham, 1991). A keystone species for northern peatlands is *Sphagnum* moss (van Breeman, 1995) with this genus of plant storing the most carbon of any other genus, dead or alive. (van Breeman, 1995). The Canadian Wetland classification system recognizes three peatland types: bog, fen and swamp. Bogs and fens are characterized by ground mosses that vary in species depending on the ground level microtopography. Along with water table proximity to ground surface, these are the main factors affecting moss species distribution in these ecosystems (Vitt, 1990).

As drought frequency and intensity increase due to climate change (IPCC, 2007), water table positions are expected to be lower (Roulet *et al.*, 1992), making peatlands more susceptible to moss stress, peat decomposition and combustion as the size of the unsaturated zone increases (Kettridge and Waddington, 2014). A reduction in water table position, surface-wetness, and near-surface wetness are the major factors affecting the carbon dioxide and methane exchange between peatlands and the atmosphere (Dise *et al.*, 1993; Harris *et al.*, 2005). Water

content has been shown to be a strong predictor of *Sphagnum* productivity (Williams and Flanagan, 1996) with sharp declines in productivity as *Sphagnum* shoots dry due to cellular damage to chlorophyll pigments (Gerdol *et al.*, 1996). This reduction in moisture limits *Sphagnum* production rates, which in turn reduces the carbon sequestration by *Sphagnum* (Thompson and Waddington, 2008) and the ecosystem.

The majority of carbon sequestration and accumulation in these peatlands is characterized by the extremely recalcitrant litter of peat moss (Gerdol and Vincentini, 2011). These recalcitrant compounds are difficult to degrade biologically (Providenti *et al.*, 1993), causing decomposition rates to be low. Saturated conditions also reduce decomposition rates, which enables peat to accumulate as production outweighs decomposition (Clymo and Hayward, 1982).

When drought occurs, peatlands can potentially maintain wet conditions through the majority of the peat profile as *Sphagnum* can lower evaporative loss, holding onto water under high surface tension conditions (Kettridge and Waddington, 2014). If the water table drops too low, past a threshold, the ability of *Sphagnum* to draw water up through capillary rise will be reduced, lowering the water supply rate from the saturated zone to the surface, which in turn will reduce evaporative loss even further (Waddington *et al.*, 2015). When the water table is at or near the surface, the evaporative demand can be high. High evaporation rates can lower the temperature of the peat surface below the air temperature (Kettridge and

Waddington, 2014). Peatlands rely on these negative feedbacks to sustain ecosystem functioning in a range of environmental conditions (Waddington *et al.,* 2015).

It has previously been shown that measurements of spectral reflectance can be used to detect the effects of chlorophyll fluorescence (Zarco-Tejada, 2002) and changes in moss water content (Van Gaalen *et al.*, 2007). By implementing remote sensing techniques, it may be possible to identify stress on larger temporal and spatial scales within chlorophyll activity even before there is a visible change in chlorophyll content (Zarco-Tejada, 2002). Thermal imaging has previously been used to monitor plant stress (Chaerle and Van Der Straeten, 2000). If leaves or vegetation are stressed, they will have less absorption (more reflection) by pigments in the visible spectrum (red, green, and blue) (Carter, 1993), and this is also characteristic of *Sphagnum* moss. The hyaline cells of *Sphagnum* can absorb water rapidly, but if they are emptied, possibly due to drought, they often turn white, which in turn causes the peatland albedo to increase (van Breeman, 1995). This white appearance is known as *Sphagnum* bleaching (Harris *et al.*, 2005) and can further reduce evaporative loss from the surface, acting as a negative feedback to water table drawdown (Waddington *et al.,* 2015).

Spectral indices based around NIR have been previously used to monitor specific *Sphagnum* species. These indices were only able to monitor the differences in 'health' (stress level) within a given species due to the difference in canopy

morphology between *Sphagnum* species (Harris *et al.*, 2005). By drying and re-hydrating *Sphagnum* samples, Harris *et al.* (2005) found a hysteretic response in two NIR indices, which suggests that the time at which images are acquired may be a very important aspect when using remote sensing on peatlands.

Additionally, the spectral signature of a peatland can be heavily dependent on the presence and abundance of overstory vegetation. Depending on the abundance of overstory vegetation, such as *Rhododendron groenlandicum* or *Chamaedaphne calyculata*, the moss may be the most dominant species, having the largest influence on the spectral signal of the peatland. Alternatively, the moss may just be part of the background, having little to no effect on the spectral signature (Vogelmann and Moss, 1993).

Given the increase in peatland disturbance and the advances in remote sensing approaches to examine the 'health' status of vegetation, the major objective of this study is to determine the remote sensing techniques that can be quickly and accurately applied to monitor peatlands from low-level platforms such as unmanned aerial vehicles (UAVs). By looking at the water content and 'health' status of peatlands at different times throughout the summer, the usefulness of VIs and thermal imaging was assessed.

2.2 METHODS

2.2.1 *Study Site*

The Near Northern Ontario Barrens & Bogs Experimental Landscape (NOBEL) (Figure 2.5.1) is located ~7 km north of Nobel, Ontario. It is part of the Canadian Shield and was previously subjected to heavy glaciation (Kolenosky and Johnston, 1967). The NOBEL is in an area classified as having a humid continental climate. The precipitation and temperature in the area are largely influenced by the Great Lakes (Kolenosky and Johnston, 1967). With an average elevation of 174 m above sea level, the average yearly temperature is 5.8 °C with extremes ranging from -39.0 °C to 37.6 °C. The NOBEL receives approximately 965 mm of rain with 302 cm of snow. The month of July receives the least monthly precipitation on average (55 mm).

The NOBEL is characterized by open gneiss rock barren ridges, which generally run west to east. The rock barren surface has been differentially eroded creating various depressions in the area (Culshaw *et al.*, 2004), which can fill with soil (predominantly organic) of varying thickness. Within these depressions, species of *Sphagnum* and *Polytrichum* moss have colonized and become the dominant species. At the edge of these depressions, the *Sphagnum* moss can be present on the rock with no mineral soil, while the middle of the depression can have anywhere from a few centimeters to over 1.5 meters of peat accumulation.

2.2.2 *Fieldwork*

Depressions in NOBEL were selected based on moss species composition and distribution within a depression (edge or middle). They were not specifically chosen based on peat depth (range 0.05 m to >1.0 m). As such, this meant moss cushions were under dynamic environmental conditions allowing for the study of potential stress on these species. The species included *Sphagnum papillosum*, *Sphagnum capillifolium*, *Sphagnum angustifolium*, and *Sphagnum fuscum*. 42 of these plots (0.2 m x 0.2 m) were established (10 *S. papillosum*, 10 *S. capillifolium*, 10 *S. angustifolium*, 2 *S. fuscum*, and 10 mixed plots) to allow for continued monitoring throughout the summer.

For photography and GIS purposes, the boundaries of the plots were distinguished by placing markers (poker chips attached to a thin metal flagpole) at the four corners of the plots. Volumetric moisture content, surface temperature, 0.05 m depth moss/peat temperature, moss chlorophyll fluorescence, and moss surface spectral reflectances were measured within each individual plot. Moisture measurements for the top 0.03 m and 0.06 m were made using a Delta-T Devices HH2 Moisture Meter and a Theta Probe ML3, which measures in electrical conductance (mV). Moss surface temperature was measured using a FLIR One Thermal Imaging Camera, which is accurate to 0.1 °C, while 0.05 m moss temperature was measured using an Oakton Thermocouple thermometer. Chlorophyll fluorescence was measured by first dark adapting samples for at least

20 minutes, and then using a handheld Opti-Sciences OS30p$_+$ Chlorophyll Fluorometer. This device measures the maximum quantum yield (F_v/F_m) by first measuring the minimal fluorescence (F_o), and then exposing the sample to a high light intensity saturation flash and measuring the maximal fluorescence (F_m). Variable fluorescence (F_v) is the difference between F_m and F_o. These measurements are made by measuring the light intensity coming off of a sample, before and after pulsing it with an array of red LEDs situated around 660nm. Spectral reflectance measurements were taken using three different Canon Rebel t3i digital cameras. The first camera was used to take normal digital photos (*i.e.* photos in the red, green, and blue wavelengths), with the other two cameras having had their internal sensors changed to view in the near-infrared and UV-A wavelengths. These measurements were repeated numerous times throughout the summer of 2015.

In ArcGIS, the images were overlaid on top of each other using the poker chips to georeference one image onto another and a tool created in ModelBuilder was used to calculate various vegetation indices (VI). The model calculates the VI, clips it to only include the moss within the plot itself and then averages this number so that each plot only has one number per VI at any time. The VIs included the Normalized Difference Vegetation Index (NDVI), the Green NDVI (GNDVI), and the Enhanced NDVI (ENDVI). The NDVI can be described by:

$$\mathrm{NDVI} = \frac{\rho_{\mathrm{NIR}} - \rho_{\mathrm{R}}}{\rho_{\mathrm{NIR}} + \rho_{\mathrm{R}}} \quad (1)$$

where ρ_{NIR} is the reflectance in the near-infrared wavelength range and ρ_R is in the red wavelength range. The GNDVI replaces ρ_R with ρ_G (reflectance in the green wavelength range) and is calculated using:

$$\mathrm{GNDVI} = \frac{\rho_{\mathrm{NIR}} - \rho_{\mathrm{G}}}{\rho_{\mathrm{NIR}} + \rho_{\mathrm{G}}} \quad (2)$$

With the idea that healthy plants will reflect light in both the near-infrared and green wavelengths, the ENDVI was created and is described by:

$$\mathrm{ENDVI} = \frac{\rho_{\mathrm{NIR}} + \rho_{\mathrm{G}} - (2 * \rho_{\mathrm{B}})}{\rho_{\mathrm{NIR}} + \rho_{\mathrm{G}} + 2 * \rho_{\mathrm{B}}} \quad (3)$$

where ρ_B is the reflectance in the blue wavelength range.

At the end of the summer, surface samples of *S. papillosum*, *S. capillifolium*, and *S. angustifolium* from this study area were placed in polyvinyl chloride (PVC) caps (measuring 0.1 m in diameter and 0.05 m in height) to conduct a lab experiment. Some extra surface samples were used to calibrate the Theta Probe and convert the electrical conductance to gravimetric water content (GWC).

2.2.3 *Laboratory Experiment*

In the laboratory, the *S. papillosum*, *S. capillifolium*, and *S. angustifolium* surface samples were wetted and given enough sunlight until they were healthy (F_v/F_m

value above 0.5). They were then placed in a Conviron E7 Reach-In Plant Growth Chamber with a CMP 6050 Control System, which allows for temperature, light, and humidity control. The chamber was set to have a constant light intensity and temperature of 22 °C. Whilst in the growth chamber, the samples were allowed to freely evaporate. The samples were then measured periodically for gravimetric water content, surface temperature, spectral reflectance and chlorophyll fluorescence (as explained above). At the end of the experiment, when all samples had reached a steady weight, they were placed in an oven for 48 hours at 65 °C to determine a dry weight. Using the same approach as before within ArcGIS, the VIs were calculated for all measurement times for each of these samples.

2.2.4 *Statistical Analyses*

Once the surface temperature data and VI data had been gathered, the *Sphagnum* was organized into two groups; 'healthy' *Sphagnum* (F_v/F_m at or above 0.2) and stressed *Sphagnum* (F_v/F_m below 0.2). To determine if there was a statistical difference between the two groups, a Student's *t*-test (Ruxton, 2006) was used. If the larger standard deviation of the two groups was more than twice as large as the smaller standard deviation, an unpooled Student *t*-test was used, otherwise a pooled Student *t*-test. By using the *t* statistic and the degrees of freedom, a p-value can be estimated using a *t*-table. If the Student *t*-test determined that the

groups were statistically different, the mean and standard deviations were used to calculate where the break between the groups occurs.

2.2.5 *Large Scale Plots*

Within a bog in the NOBEL, two 5 m x 10 m plots were set up using flags and poker chips in a grid system. Using the Chlorophyll Fluorometer, the 'health' status of these plots was measured by assessing the maximum quantum yield at every meter along the north and south boarders, approximately 0.5 m in (n = 20). The digital cameras were then attached to a 3 m long telescopic camera pole allowing for RGB, NIR, and UV-A images to be captured from above of the plot. Using the poker chips as a guide, these images were stitched together and overlaid on top of each other to create a single raster dataset. This was conducted on June 17th and August 6th for both plots representing a dry and a wet period.

2.3 RESULTS

2.3.1 *Temperature and Moisture*

In the NOBEL, *Sphagnum* moss had a wide range of surface temperatures, ranging anywhere from 5 °C to 40+ °C in the summer months. When the surface temperature rises above 30.8 °C ($p < 0.0001$), the chlorophyll fluorescence value becomes low (F_v/F_m is close to 0) (Figure 2.5.2a). *Sphagnum* can also have a very wide range of moisture contents in the field, having a GWC as high as 42 g/g, and

a low of 1.75 g/g. A low surface moisture content did not necessarily mean that the F_v/F_m was low (Figure 2.5.2b), however, when the GWC of *Sphagnum* at the surface is above 10 g/g, the F_v/F_m was high (above 0.38).

In the summer of 2015, *Sphagnum* in this region had wet antecedent moisture conditions (Figure 2.5.3b). On May 19th, the *Sphagnum* had an average GWC of 19.8 g/g, however, this started to decrease, decreasing to 12.5 g/g by June 6th, and 14.2 g/g on June 24th. July was a very dry month (36.9 mm of rain in total), and by August 7th, the average GWC of *Sphagnum* was 5.9 g/g. The GWC remained relatively constant throughout August, dropping slightly to 5.6 g/g by August 15th, and then rising minimally to 7.9 g/g by August 23rd. Within these boxplots, for each day, it is important to remember that these measurements were taken at different times of the day. Some of the earlier measurements in the day will have a higher moisture content because of dew, as well as a lower surface temperature and higher chlorophyll fluorescence.

The surface temperature of *Sphagnum* (Figure 2.5.3c) had a steady rise throughout the summer. The average surface temperature was 16.4 °C on June 6th, increasing to 30.2 °C by August 15th and then decreasing slightly to 26.5 °C by August 23rd. The F_v/F_m of *Sphagnum* (Figure 2.5.3a) was high during the first summer months (above 0.6 on average in May and June) and by August 7th it had decreased to 0.19 on average. After this, the average F_v/F_m for *Sphagnum* started to rebound, reaching 0.37 by August 23rd.

2.3.2 *Laboratory Experiment*

In the laboratory, the surface temperature of *Sphagnum* ranged from 15.3 °C to 22.2 °C (Figure 2.5.4a). When the temperature was lower, *Sphagnum* had a higher F_v/F_m (above 0.2), whereas, when the surface temperature rose above 18.2 °C ($p < 0.0001$), the *Sphagnum* had a low F_v/F_m value (below 0.2). When *Sphagnum* had a low GWC (below 5 g/g), it had a low F_v/F_m (Figure 2.5.4b), however, when the GWC was high (above 5 g/g), the F_v/F_m was also high, indicating the presence of a threshold between 'healthy' and stressed *Sphagnum*. When *Sphagnum* had a high GWC, the evaporation rate from the sample was equal to or greater than the potential evaporation (4 mm/day), and as the GWC decreased below 9 g/g the ration rate was hindered by *Sphagnum* attempting to retain as much water as it could (Figure 2.5.4c).

2.3.3 *Utilizing Remote Sensing*

In the field, the NDVI (Figure 2.5.5a) shows little separation between *Sphagnum* with low F_v/F_m or a high F_v/F_m ($p > 0.05$). The calculated NDVI value for these plots was always between 0 and 0.35. The GNDVI (Figure 2.5.5b) had a range from 0.25 to 0.54, and showed separation ($p < 0.05$) between *Sphagnum* with low and high F_v/F_m values, but only within most of the individual *Sphagnum* species and not *Sphagnum* as a whole. This separation occurred at a GNDVI value of 0.31 for *S. angustifolium*, 0.3 for *S. papillosum*, and 0.35 for *S. fuscum*, and there was no clear break for *S. capillifolium*. The ENDVI (Figure 2.5.5c), ranging from

-0.03 to 0.42, showed the best separation ($p < 0.0001$) between *Sphagnum* as a whole between *Sphagnum* with a low F_v/F_m and *Sphagnum* with a high F_v/F_m. For all *Sphagnum* species studied, this break occurred at 0.11, where an ENDVI value above this value indicates a high F_v/F_m, and a value below indicates a low F_v/F_m.

In the laboratory, the NDVI, ranging from -0.64 to -0.08, showed minor separation ($p < 0.001$) between *Sphagnum* with low F_v/F_m and *Sphagnum* with high F_v/F_m (Figure 2.5.6a). When looking at the individual species, there was better separation, but there was overlap between where *Sphagnum* with a low F_v/F_m ended and where *Sphagnum* with a high F_v/F_m began. The GNDVI (Figure 2.5.6b), ranging from -0.58 to 0.46, had very well defined separation ($p < 0.0001$), however, this did not occur at the same value for all *Sphagnum* species. For *S. angustifolium*, this break occurred at -0.35, at -0.22 for *S. papillosum*, and -0.07 for *S. capillifolium*. The ENDVI (Figure 2.5.6c), ranging from -0.23 to 0.12, showed a clear break for all *Sphagnum* species at -0.12 ($p < 0.0001$), where if the ENDVI was below this value, the *Sphagnum* had a low F_v/F_m and above this value, the *Sphagnum* had a high F_v/F_m.

2.3.4 *Large Scale Application*

On June 17th, Plot 1 (Figure 2.5.7) and Plot 2 (Figure 2.5.8) had groundcover dominated by *Sphagnum* moss with high F_v/F_m. At this time, Plot 1 had an average F_v/F_m of 0.57, and median of 0.56, while Plot 2 had an average of 0.61, and median of 0.64. By August 6th, these had decreased to averages of 0.35 and

0.50, with medians of 0.41 and 0.59 respectively. In Plot 1, the ENDVI decreased on average by 0.07 (median decreased by 0.05), going from 0.02 to -0.05 during this period, while Plot 2 decreased on average by 0.04 (median decreased by 0.02), from 0.01 to -0.03.

2.4 DISCUSSION

In both the field and laboratory, the results suggest that the NDVI does not effectively estimate the 'health' of *Sphagnum* moss. Most vegetation indices, including both the NDVI and the GNDVI, were developed primarily to indicate changes that are characteristic of green vegetation (Jones and Vaughn, 2010). However, *Sphagnum* can have various colours depending on the sphagnorubin content of the species (Letendre *et al.*, 2008). Sphagnorubin can cause a reflectance peak in the red wavelength region, resulting in a more red appearance (Rudolph and Jöhnk, 1982; Letendre *et al.*, 2008). Spectral indices derived from NIR have been shown to be highly correlated with near-surface moisture, however a hysteretic effect has been observed between the two (Harris *et al.*, 2005). As this NIR index follows a hysteretic curve, alone, it may not accurately portray the chlorophyll activity. The NDVI data presented here show that the F_v/F_m of *Sphagnum* and NDVI may also be following a hysteretic curve. Although Harris (2008) found that the NDVI was able to monitor changes in the canopy morphology of *Sphagnum* and was indirectly correlated with the photosynthetic

activity; if the NDVI and F_v/F_m are following a hysteretic curve, then the NDVI is unsuitable to accurately monitor changes in chlorophyll content as the same NDVI value can indicate both *Sphagnum* with high or low F_v/F_m depending on which side of the curve it currently is on.

Moreover, the GNDVI, which uses the difference in the green wavelength range, has been used to monitor the rate of photosynthesis and has been found to be five times more powerful than the NDVI to monitor plant stress by sensing the concentration of chlorophyll-a (Gitelson *et al.*, 1996). The NDVI and the GNDVI have been shown to be very similar for monitoring nitrogen content in vegetable crops (Padilla *et al.*, 2014). For *Sphagnum* moss, because there is an offset between species in terms of the GNDVI value where *Sphagnum* chlorophyll-fluorescence shuts down, the GNDVI could potentially be used to monitor stress, provided that the distribution of the species can be mapped using remote sensing or is already known. From the data presented here, the GNDVI may have a slight hysteretic curve, however, it is less prominent than the one produced by the NDVI and as such provides a better indication of the *Sphagnum* 'health' status.

Wang *et al.* (2007) found that by adding the blue band into the GNDVI to create a Green-Blue NDVI, they could make better estimations for the LAI of rice. Using either 550 ± 20 nm (green) or 715 ± 20 nm (red edge), 450 ± 20 nm (blue), and the NIR band above 750 nm is sufficient in estimating chlorophyll content (Gitelson *et al.*, 2003). The ENDVI, which utilizes both green and blue, along

with NIR, had results that were not specific to any of the species examined here (*S. papillosum*, *S. capillifolium*, *S. angustifolium*, and *S. fuscum*), but instead, the threshold between high and low F_v/F_m for all *Sphagnum* species occurred around the same ENDVI value. This single threshold among all of the species suggests that the ENDVI can be used to monitor the stress of *Sphagnum* without prior knowledge of the distribution of each species on a larger scale. By using this method, it allows for a quick determination of the 'health' status (F_v/F_m) for *Sphagnum* moss (*i.e.* if ENDVI is below the threshold value, the *Sphagnum* moss is stressed, and *vice versa*).

At the beginning of the summer of 2015, *Sphagnum* moss in NOBEL had an abundant amount of water. As the summer progressed, *Sphagnum* lost water that was at or near the surface due to evaporation from an increase in ambient temperature and solar radiation. As the moisture content of *Sphagnum* drops below an optimum level, the productivity declines sharply as water drains from the chlorophyllose cells (Gerdol *et al.*, 1996; Thompson and Waddington, 2008). *Sphagnum* relies on this availability of water to be productive, so when water limitation occurs the chlorophyll in *Sphagnum* shuts down (indicated by a low F_v/F_m). The water lost due to evaporation helps mitigate the surface temperature increase of the *Sphagnum* moss. Kettridge and Waddington (2014) found that as the evaporative demand increases, evaporation keeps the surface temperature of peat below the air temperature. Peatlands have the potential to reduce evaporation under extreme drought conditions to maintain saturated conditions, helping to

reduce decomposition throughout the majority of the peat profile. Once the moisture drops low enough, where the peatland will reduce evaporation and the *Sphagnum* is unable to draw more water up from the water table, the surface temperature will increase far above ambient (Kettridge and Waddington, 2014). High peatland surface temperatures under such field conditions have been associated with a large reduction in peat evaporation (Kettridge *et al.*, 2012). Kellner (2001) found that there could be up to an 8 °C difference between the *Sphagnum* surface temperature and the ambient temperature due to this process, however, in this study, it is shwon that the *Sphagnum* surface temperature can reach up to 12 °C higher than the ambient temperature. In the laboratory, there is a clear threshold between temperatures when *Sphagnum* has active chlorophyll (high F_v/F_m) and when its chlorophyll is inactive (low F_v/F_m). This break is very well defined in the laboratory and occurred at 19 °C, but this is not the case for the field. In the field, where *Sphagnum* still has some connectivity to the water table, this break occurs around 30 °C and is not as clearly defined, possibly due to the current level of connectivity the moss at the surface has with the water table.

When *Sphagnum* moss has an abundance of moisture available, water at the surface will evaporate at a rate that is greater than an open water surface. Nichols and Brown (1980) found that evaporation from *Sphagnum recurvum* was at a rate twice that of an open water surface at temperatures between 7 °C and 25 °C. They found that under the same environmental conditions, *Sphagnum* with a

water level at the peat surface would have a lower surface temperature than that of open water. The data presented here, shows that in a controlled laboratory, the evaporation rate from *S. angustifolium*, *S. papillosum*, and *S. capillifolium* was between 1 and 1.75 times that of an open water source when the GWC of the *Sphagnum* was above 9 g/g. Below this GWC, not only does the evaporation rate decrease due to water limitations, but this is also the GWC when the chlorophyll of *Sphagnum* shut downs and the *Sphagnum* is no longer photosynthesizing.

There is concern for peatland carbon stocks due to their vulnerability to decomposition and combustion with low water table positions (Kettridge and Waddington, 2014) as drought frequency and intensity have increased within Ontario (Faulkenham *et al.*, 2003). Using remote sensing for timely and accurate change detection allows for a better understanding of the relationships and interactions across the landscape (Lu *et al.*, 2004; Coppin *et al.*, 2004). The changes in a landscape are more strongly related to changes shown by vegetation indices than compared to single bands (Coppin *et al.*, 2004) and so vegetation index differencing could potentially be used to select a threshold to indicate changed areas (Lu *et al*., 2004). The threshold shown in the ENDVI in both the field and laboratory data presented here could be used to indicate these changed areas as its threshold shows a clear break between healthy and stressed *Sphagnum*.

From the data presented here, thermal imaging, such as using a FLIR camera, or the ENDVI can be used to monitor the 'health' status of *Sphagnum* moss using

remote sensing. By combining the two methods, it may also be possible to not only monitor the stress of *Sphagnum*, but with some confidence be able to monitor if the current stress is being caused by water limitations or not. These methods also allow for the distribution of stress and productivity to be estimated or modelled within peatlands.

2.5 FIGURES

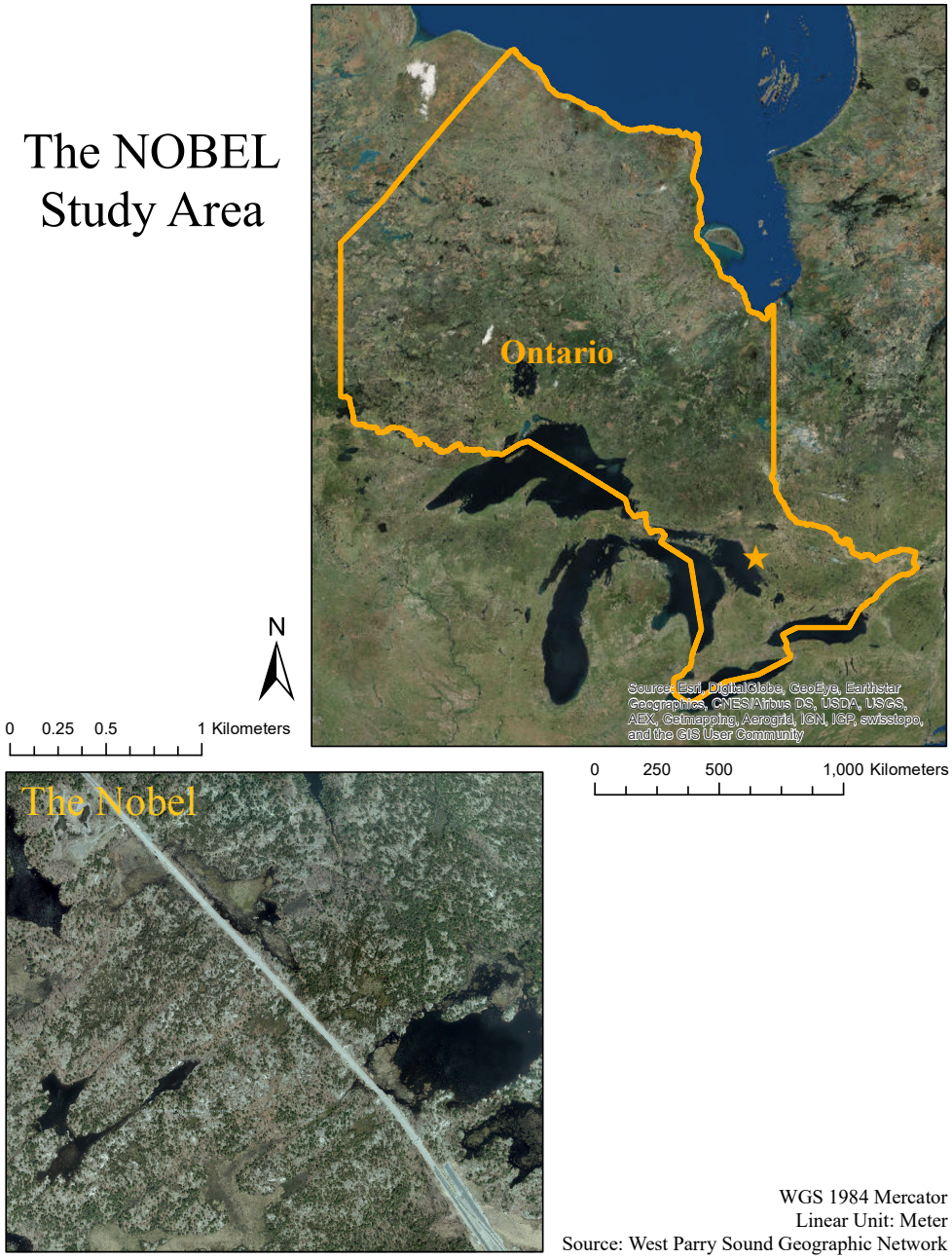

Figure 2.5.1: Map of the NOBEL

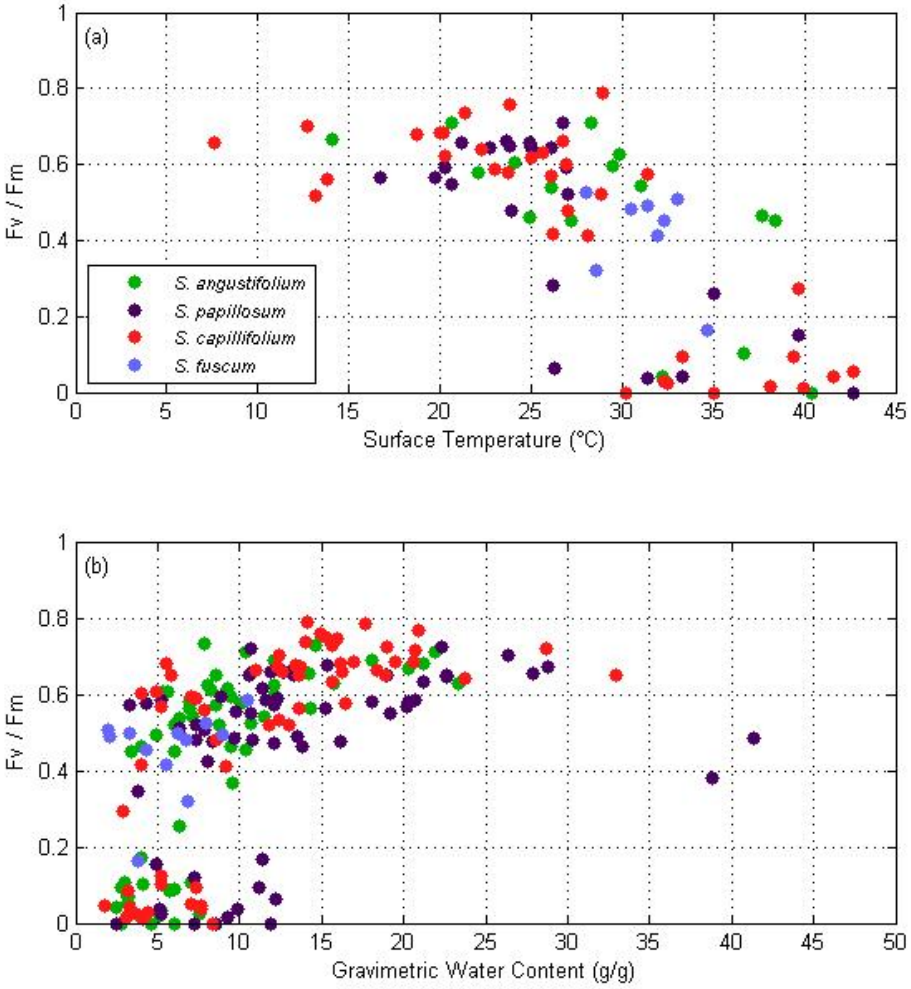

Figure 2.5.2: NOBEL field data showing (a) the effects of surface temperature (only non-shaded plots are included), and (b) surface moisture content on chlorophyll-fluorescence.

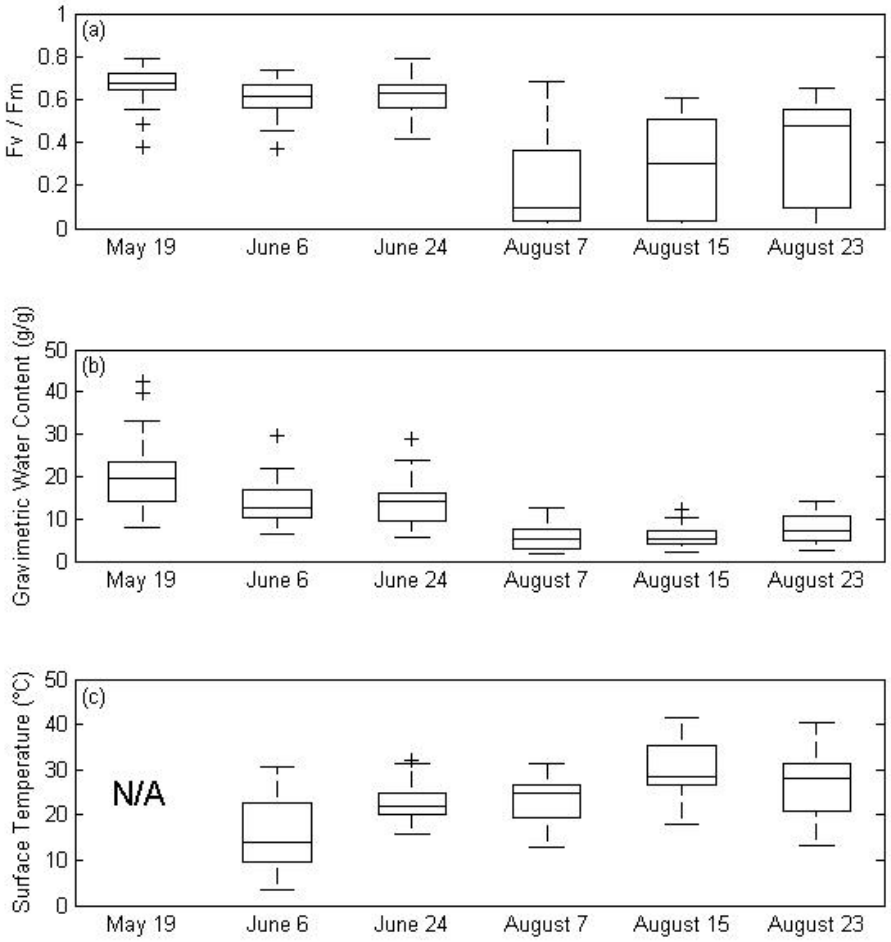

Figure 2.5.3: Representation of how (a) chlorophyll-fluorescence, (b) surface moisture content, and (c) surface temperature changed throughout the summer of 2015.

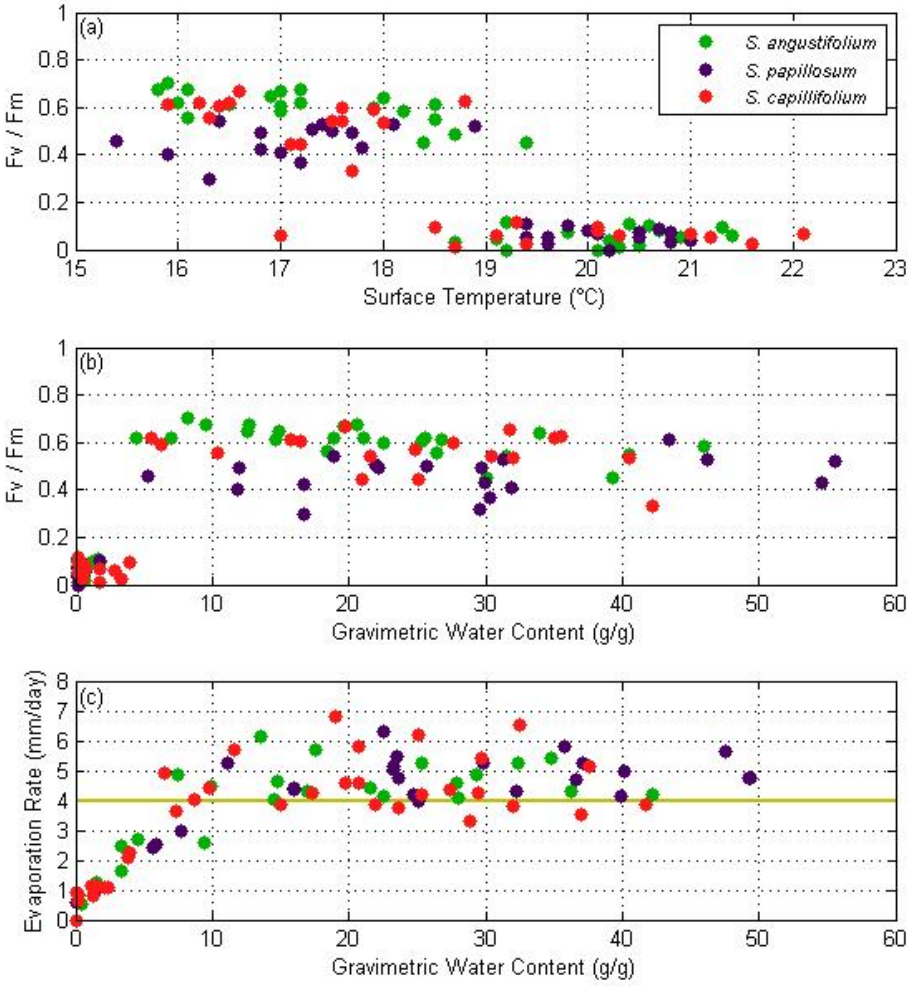

Figure 2.5.4: Laboratory data showing the effects of (a) surface temperature and (b) surface moisture content on chlorophyll-fluorescence, and (c) depicts the evaporation from the *Sphagnum* samples at various moisture contents, where the yellow line shows potential evaporation.

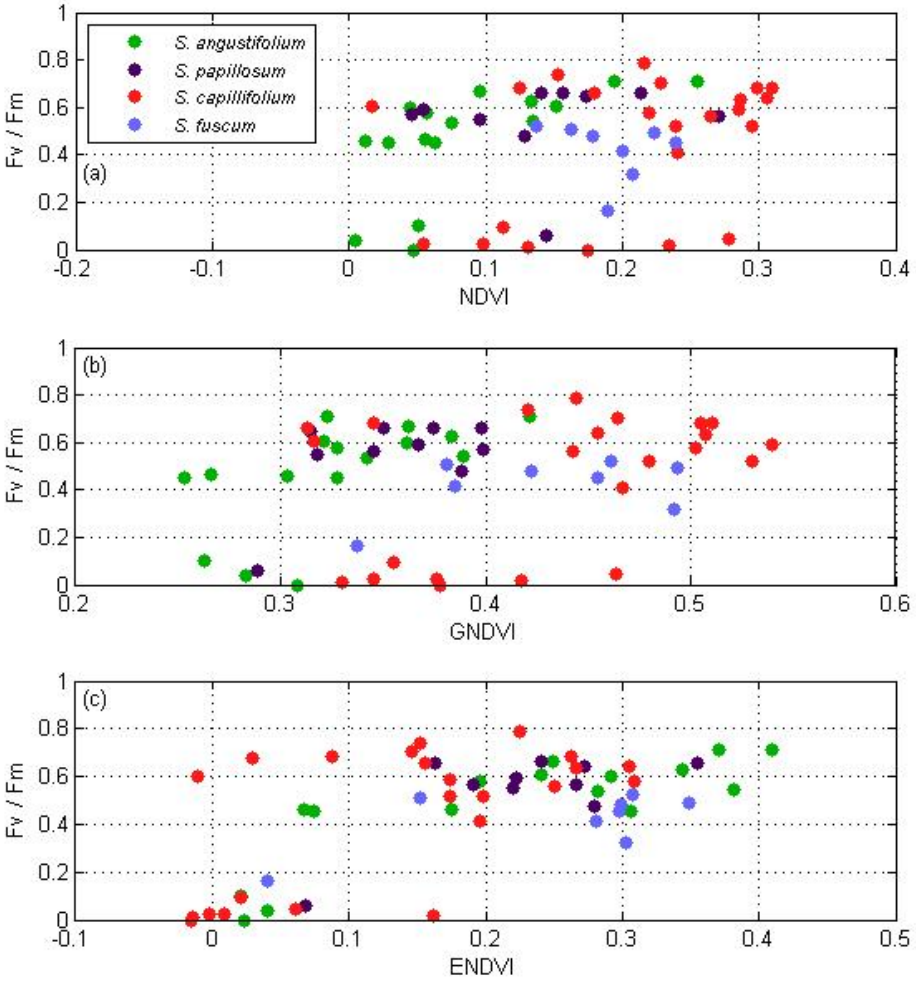

Figure 2.5.5: NOBEL field data showing chlorophyll-fluorescence with the (a) NDVI, (b) GNDVI, and (c) ENDVI.

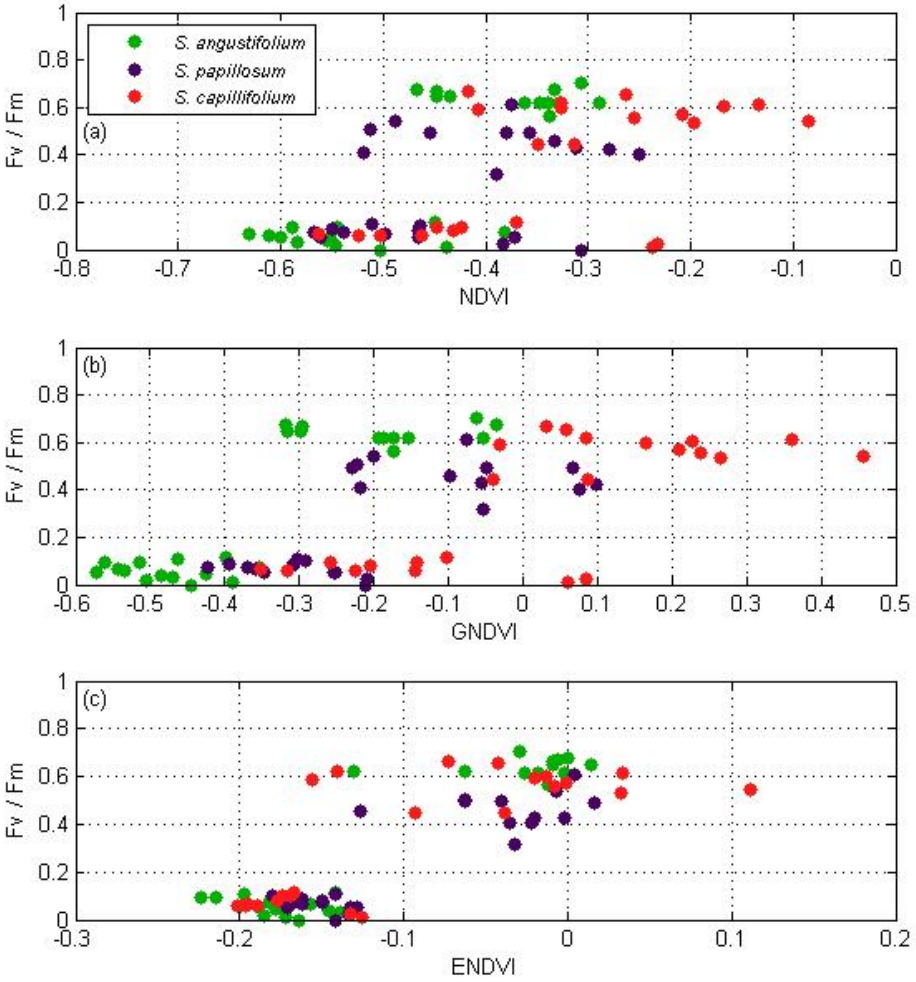

Figure 2.5.6: Laboratory data showing chlorophyll-fluorescence with the (a) NDVI, (b) GNDVI, and (c) ENDVI.

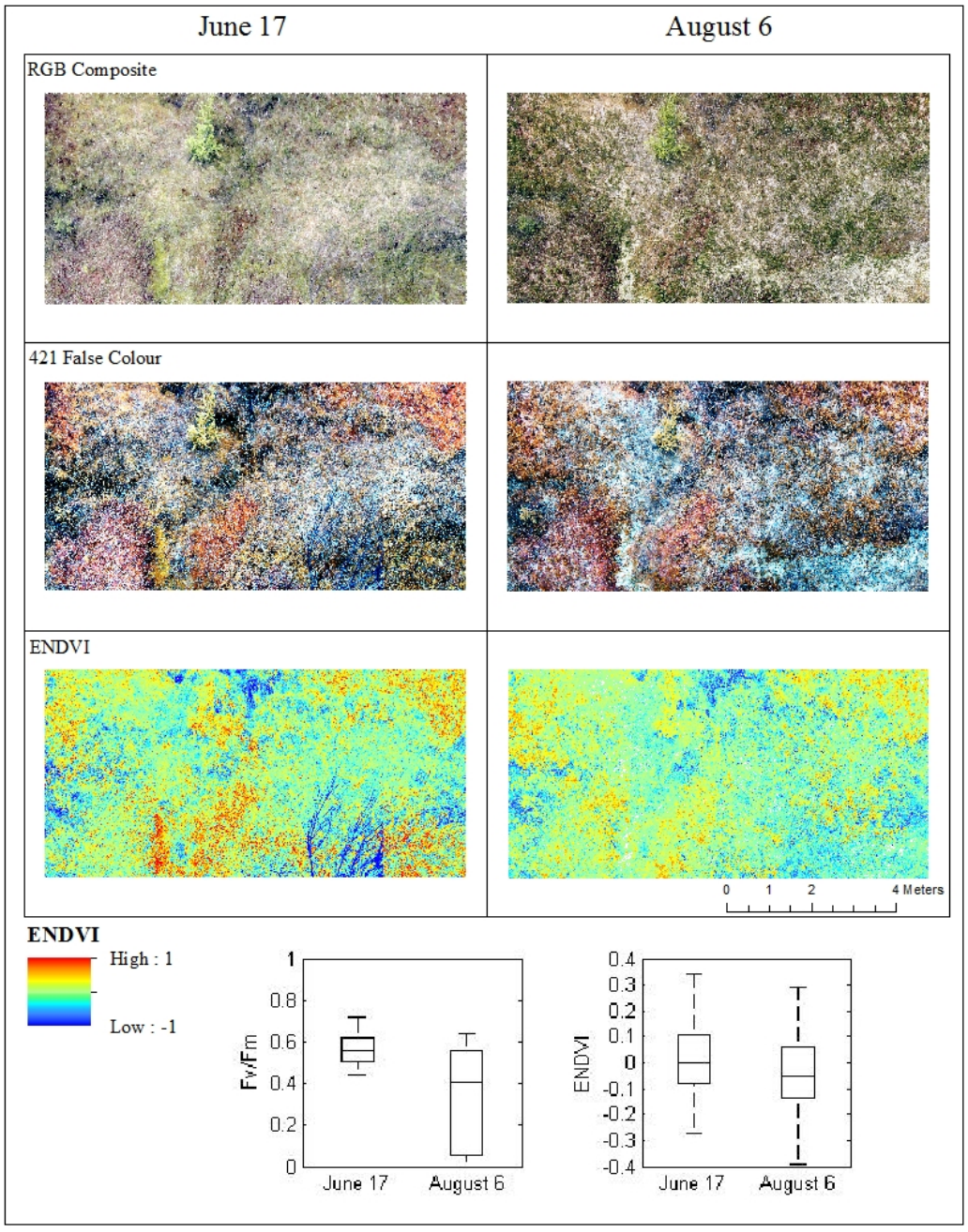

Figure 2.5.7: Depiction of the change detection in Plot 1, in the RGB composite (top), NIR-G-B composite (second), and the ENDVI (third). The bottom graphs show the change in chlorophyll fluorescence (left) and the ENDVI statistics (right).

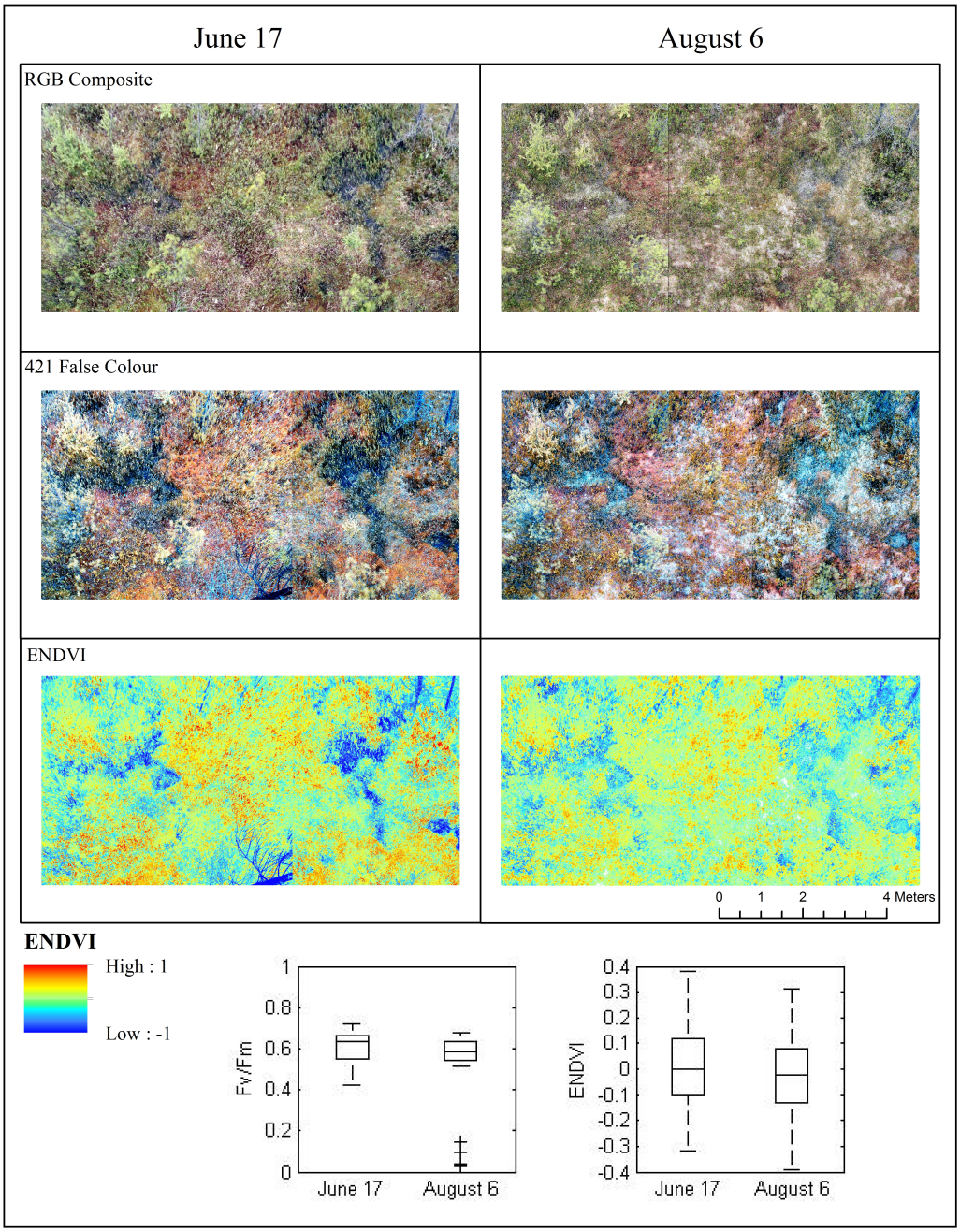

Figure 2.5.8: Depiction of the change detection in Plot 2, in the RGB composite (top), NIR-G-B composite (second), and the ENDVI (third). The bottom graphs show the change in chlorophyll fluorescence (left) and the ENDVI statistics (right).

CHAPTER 3: UTILIZING REMOTE SENSING TO MONITOR POST-FIRE RECOVERY IN PEATLANDS

3.1 INTRODUCTION

In the Western Boreal Plains, wildfire is the largest disturbance in peatland ecosystems (Turetsky, 2002), accounting for 97% of the disturbance to peatlands by area (Granath *et al.*, 2016). The effect of fire on a peatland ecosystem is dependent on pre-fire conditions, including the spatial variability in species composition, and site hydrology (Benscoter and Wieder, 2003), as well as the intensity of the fire (Lukenbach *et al.*, 2015b). Hummock moss species, which have better water retention traits (Benscoter and Vitt, 2008), typically exhibit lower burn severity in comparison to hollow species, as more energy is required to drive off the moisture and ignite the organic matter (Shetler *et al.*, 2008; Kettridge *et al.*, 2012). Although wildfire within peatland ecosystems can result in the die-off of ground layer vegetation and complete stand mortality (Zoltai *et al.*, 1998; Benscoter and Vitt, 2008) they are typically considered as resilient ecosystems as they can return to a net carbon sink within 20 years of burning (Wieder *et al.*, 2009). The largest amount of ecosystem change in the first 10 years occurs within the ground layer vegetation (Benscoter and Vitt, 2008). For example, Benscoter (2006) found that *Sphagnum* mosses rarely occurred in the absence of true mosses post-fire, and that only one-third of areas with true mosses had *Sphagnum* moss as well. This suggests that for the successful re-

establishment of *Sphagnum* moss, post-fire microhabitat modification may be required (Benscoter, 2006).

After the passage of a low-severity fire, ericaceous shrubs, like *Rhodedendron groenlandicum*, also become more abundant (Foster, 1985; Nguyen-Xuan *et al.*, 2000). During a low-severity fire, these species reproductive organs are generally unaffected (Lecomte *et al.*, 2005) as they are deeply buried in the organic substrate (Flinn and Wein, 1977). Previous work has shown that after a fire, the distribution of this species is independent of the distribution of the groundcover. These ericaceous shrubs have a detrimental effect on the recolonization and growth of *Picea mariana* due to water-soluble phenolics and their ability to alter ecosystem processes such as nutrient cycling (Nilsson *et al.*, 1993; Mallik and Mallik, 1997; Lecomte *et al.*, 2005).

After a fire passes, accurate information relating to the spatiotemporal variability on impacts to vegetation is important for quantifying the impacts of the fire and monitoring restoration and recovery (Gites *et al.*, 2009). By using datasets acquired at different times, the change in biophysical environments, such as those affected by fire can be monitored using change detection techniques (Singh, 1989; Lunetta *et al.*, 2006). By using change detection, or more specifically the subtraction of images (Kasischke *et al.*, 1993), plant response to fire can be monitored by using variations in VIs to quantify the recovery rate (Diaz-Delgado and Pons, 2001). A decrease in the presence of green vegetation and vegetation

moisture causes the NIR reflectance to decrease with burn severity (Lules *et al.*, 2006; Robichaud *et al.*, 2007; Gitas *et al.*, 2009). As such, the change in NDVI has previously been shown to be a fast approach for monitoring the change in land-cover (Lunetta *et al.*, 2006). VIs, such as the NDVI, can be used over time as a surrogate to the chronosequence of vegetation recovery (Epting and Verbyla, 2005).

The major objectives of this study are to determine the best classification scheme for monitoring post-fire recovery in a peatland ecosystem, to identify the vegetation index that can best represent the ground layer vegetation of a peatland as a whole, and to identify any possible connection of broadly applying this vegetation index to monitor peatland trajectory post-fire. By using remote sensing to create a classification scheme, it allows for the analysis of spatial distribution for peatland post-fire recovery.

3.2 METHODS

3.2.1 *Study Site*

The Utikuma Lake Research Study Area (URSA) (Figure 3.5.1) is located 370 km north of Edmonton, Alberta (Hokanson *et al.*, 2015). It is located within the boreal plains with a sub-humid climate where the annual potential evapotranspiration (517 mm) often exceeds the annual precipitation (481 mm)

(Bothe and Abraham, 1993; Marshall *et al.*, 1999). In May 2011, a ~90,000 ha fire burned a large portion of the URSA (Devito *et al.*, 2012; Lukenbach *et al.*, 2015a).

In this study, the focus was placed on two sites, both of which were affected by the 2011 fire. The first is a ~4 ha bog within the lake 171 catchment (115.188W 55.982N), located on a lacustrine clay plain (CP-B) (Lukenbach *et al.*, 2015a). It is an isolated portion of a larger peatland complex, which connects to the lake (Ferone and Devito, 2004).

The second site is a ~0.5 ha bog within the lake 16 catchment (115.560W 56.106N) and is ephemerally perched above both local and intermediate groundwater flow systems. Sitting adjacent to a regional topographic high, it is located within a glaciofluvial outwash (Smerdon *et al.*, 2005; Lukenbach *et al.*, 2015a). Both sites had hummock-hollow microtopography, where hummocks were dominated by *S. fuscum*, while *Pleurozium schreberi* and *S. angustifolium* were the dominant species within the respective hollows (Lukenbach *et al.*, 2015a).

3.2.2 *Initial Plot Setup*

After the Utikuma fire in 2011, large 5 m x 20 m plots were set up in the two sites (CP-B, and EP-B), however, because EP-B slopes towards the east side of the plot and goes into the mineral upland, the analysis here was limited to the west side, a

5 m x 10 m plot instead (to ensure only bog vegetation was captured). After defining the boundaries of these plots, the vascular cover was removed in the summer of 2012 to allow for the creation of a digital elevation model (DEM). To create this DEM, a 3-dimensional model was first created from the Structure from Motion approach in MeshLab by utilizing >100 photos that had been taken of the plot from a variety of different angles and heights. This 3-D model was then scaled in ArcGIS by using control points of known distance and relative height difference to create the final DEM. This DEM layer was then converted to an aspect layer and a slope layer in ArcGIS. After having removed the vascular vegetation in 2012, the plots were then allowed to recover, undisturbed, for the next three years.

Within each plot, an extensive vegetation survey was conducted for both the ground layer vegetation and the vascular cover. The ground layer vegetation was classified using the same classification scheme as Lukenbach *et al.* (2015a). This was accomplished by using a 0.6 m x 0.6 m quadrat that had been split into 9 equal parts (0.2 m x 0.2 m) and by conducting an individual survey for all 9 of these squares at 12 locations in EP-B and 18 within CP-B.

Using a 3 m long telescopic camera pole, images of the plot were captured from above. This was conducted using 3 different cameras, all using the same body and lens (Canon rebel t3i and an EFS 10-18 mm lens). The first camera was used to take normal digital photos (*i.e.* red, green, blue), while the other two cameras

have had their internal sensors changed to view in the UV-A (300 nm – 400 nm) and NIR (680 nm – 900 nm) wavelengths. These images were then stitched together and overlaid on top of each other to create a raster dataset. To aid in the process, poker chip 'markers' were placed in a grid format within the plot before taking pictures as to more easily identify the location and orientation of each photo. This was completed on July 10th for both EP-B and CP-B.

3.2.3 *Leaf Area Index and Aboveground Biomass*

Both plots were also split into subplots that measured 1 m x 1.25 m. For each of these subplots (n = 40 for EP-B, n = 80 for CP-B), the vascular cover (dominated by *R. groenlandicum*) was clipped. This was done by keeping the plants intact and only clipping them at the base and placing them into bags to keep the plants from individual subplots together. If an individual plant was simultaneously in more than one subplot, it was separated so that the portion that was in each subplot was allocated correctly. The plants were then weighed and selectively separated into stems and leaves. The leaves were then spread across a white board, photographed and analyzed for Leaf Area Index (LAI) using a tool created in ArcGIS's ModelBuilder by converting these photos into an area value. This tool separates the white space of the board and the portion covered in leaves into two separate layers, and by using the number of pixels allocated to each of these layers and the area of the board, a LAI calculation can be made. The stems and

leaves were then dried at 65 °C for 48 hours and weighed to calculate aboveground biomass.

Using the raster dataset, and another tool created in ArcGIS's ModelBuilder, multiple VIs were calculated for each subplot. These VIs including the NDVI, the GNDVI, the ENDVI, and numerous other VIs were an average for each of the individual subplots (see Chapter 2 for NDVI, GNDVI, and ENDVI equations). This was done to create a relationship between LAI and individual VIs. A vascular classification layer was also created using an exponential transformation of the NIR band. To clean up this classification, a majority filter was used to remove lone pixels.

3.2.4 *Ground Layer Classification*

One of the major aims of this work was to generate digital layers for these plots in accordance with the classification scheme set out by Lukenbach *et al.* (2015a). This was accomplished by first creating another raster dataset where there was no vascular cover. A few days after having fully clipped both sites (July 17th), the telescopic pole and cameras were once again used, and with the same approach as before, these photos were stitched together and overlaid on top of each other to create a ground layer raster dataset. The ground layer raster dataset was then converted to a false colour image by using the difference between two bands for each of the colour inputs. For this false colour image; the new red band represented red minus green, the green band represented green minus blue, and

the new blue band represented blue minus red. Scattergram regions were then created using this false colour image to generate a moss layer.

The areas that had been classified as the moss layer were then removed from the ground layer raster dataset, so that only the areas that had yet to be classified remained. This was then used to create another false colour image; where the new red band represented NIR minus green, the new green band represented green minus blue, and the new blue band represented blue minus NIR. From this second false colour image, new scattergram region were created to generate the burned hollow (BH) and burned feather moss lawn (BFL) layers.

The moss, BH, and BFL layers were then added together to create one cohesive image. A majority filter was then used to smooth the image and redistribute lone pixels. By utilizing the data from the vegetation survey, these classified layers were tested for their level of agreement using an Error Matrix and Kappa Analysis (**$\hat{K}$**) (Landis and Koch, 1977).

The distributions of individual bands, VIs, elevation, aspect, and slope throughout the generated layers (vascular, moss, BH, BFL) were extracted using a tool in ArcGIS. This extraction allows for the analysis of these distributions between and within different layers. For individual bands, and the VIs, a One-Way Analysis of Variance (ANOVA) was used to determine if there was a statistical difference between the means of the different classes (Stoline, 1981; González-Rodríguez *et al*. 2012). By using the means and standard deviations of the distributions within

each of the classes, a Mean-Mean Multiple Comparison Display was generated to depict the degree of overlap between each of the classes (Heiberger and Holland, 2006), and give a better understanding of the ANOVA results. By using the Mean-Mean Comparison Display, a determination of overlap between two individual classes can be made, whereas an ANOVA will only determine if there is any difference between all of the groups.

3.3 RESULTS

3.3.1 *Leaf Area Index and Aboveground Biomass*

Average aboveground biomass at EP-B and CP-B was 243.1 +/- 97.6 g m^{-2} and 307.1 +/- 72.9 g m^{-2}, respectively. Assuming a 50 % carbon content for organic matter, 121.5 g C m^{-2} and 153.5 g C m^{-2} had accumulated over the three year period for EP-B and CP-B, respectively. Assuming a constant growth rate, this represents a net primary productivity value of 40.5 g C m^{-2} yr^{-1} and 51.2 g C m^{-2} yr^{-1} for EP-B and CP-B, respectively. Assuming the plots are representative of their respective sites (the peatland as a whole) and given the areas of these peatlands (EP-B = 0.5 ha, CP-B = 4 ha; Lukenbach *et al.*, 2015a) total net primary production for EP-B and CP-B was 202.5 kg C yr^{-1} and 2048 kg C yr^{-1}, respectively for the aboveground vascular vegetation.

Within these peatlands, there is a linear relationship between the amount of dry organic matter per m^2 and the LAI (Figure 3.5.2a; $R^2 = 0.814$, $p < 0.001$). There is also an exponential relationship between the ENDVI average of the subplots and the LAI value (Figure 3.5.2b). Three different VIs were tested, such as the NDVI ($R^2 = 0.077$, $p = 0.0241$), and the GNDVI ($R^2 = 0.530$, $p < 0.001$), however, the ENDVI provided the best relationship with LAI ($R^2 = 0.687$, $p < 0.001$). This relationship along with the raster dataset can be used to create a predicted LAI spatial distribution map (Figures 3.5.3 and 3.5.4). EP-B has higher LAI values, with some points reaching as high as 3.3 and an overall average for the plot of 0.65, whereas CP-B is more well distributed, only reaching as high as 2.15, but with a higher overall average LAI of 1.2.

3.3.2 *Supervised Classification*

The classification scheme for both CP-B (Figure 3.5.3) and EP-B (Figure 3.5.4) show a large difference in percent cover of moss and BFLs. Moss covers only 13.0% of the plot in EP-B and 25.1% in CP-B; while the BFLs coverage was 48.1% and 36.6%, respectively; and BH coverage was 38.9% and 38.3%, respectively. The classification scheme provided an overall accuracy of 77.0% for CP-B and 84.0% for EP-B from their individual error matrices (Table 3.5.11 for CP-B and Table 3.5.12 for EP-B). From these error matrices, a $\hat{\mathbf{K}}$ value of 0.627 for CP-B and 0.714 for EP-B were calculated. These values suggest that there is a substantial agreement between the classification scheme and the

vegetation survey (Landis and Koch, 1977) and that the classification is significantly better than using a random classification scheme (Congalton and Green, 2009; Jin, 2014). In EP-B, the User's Accuracy for the moss layer is only 50.0%, even though the Producer's Accuracy is 80.0% for this layer. This low User's Accuracy can be attributed to the lack of moss within the plot and that the vegetation survey located a lot more BFL within this plot. In CP-B, where there is moss, the exact same classification scheme had a User's Accuracy for the moss layer of 84.9%, while the Producer's Accuracy was 78.6%.

3.3.3 *Band and Vegetation Index Distributions*

The vascular plants (dominated by *R. groenlandicum*) are the most reflective layer in these peatlands. The average digital number of the vascular layer for the red band is 155.5 between both sites (Figure 3.5.5 and Figure 3.5.6), 243.5 for the NIR band, and 229.5 for the UV-A band. Moss is the second most reflective layer with 150.5 for the red band, 212.5 for the NIR band, and 223 for the UV-A band. BH and BFL reflectances are similar with both having an average digital number of 118.5 for the red band between both sites, 146.5 and 147.5 respectively for the NIR band, and 178 and 185 respectively for the UV-A band. From the One-Way ANOVA and the Mean-Mean Multiple Comparisons test, the NIR and UV-A bands provide the best separation between the individual classes.

The VIs did not all have the same type of trend (Figure 3.5.7 and Figure 3.5.8). The NDVI had an average between both sites for Moss and BH that were 0.13 and

0.125 respectively. The GNDVI had an average of 0.29 for the vascular layer, followed closely by BH at 0.285. The ENDVI gave the best separation between classes, where the vascular layer had an average value of 0.245, Moss had an average of 0.075, BH had an average of 0.03, and BFL had the lowest average of -0.055 between both sites. The spatial distribution of ENDVI across the plots can be observed in Figure 3.5.2 and Figure 3.5.3. In both of these images, it is apparent that among the ground cover layers (i.e. Moss, BH, and BFL), the higher ENDVI values occur where the moss is more prevalent.

3.3.4 *Elevation and Aspect*

In CP-B, BH groundcover exists at elevations between 0 m and 0.3 m, while the top of hummocks are dominated by moss (Figure 3.5.9a), although moss is also growing at lower elevations (30% of the moss is below 0.25 m). The BFL groundcover in CP-B is more evenly distributed, occurring at high and low elevations within the plot. In EP-B (Figure 9c), these same trends would not be expected as the plot is sloping strongly towards the margin (the East). In this plot, only 17.7% of moss and 15.3% of BFL are above the highest BH.

Comparing the aspect distributions for CP-B (Figure 3.5.9b) there is a higher percentage of moss growing on north facing aspects, while there is a higher tendency for BFLs to be on south facing aspects, while BHs are spread evenly among all aspects. The distributions of aspect for EP-B (Figure 3.5.9d) show no tendency for any of the classes to exist in any particular orientation.

Although each class can exist facing any direction, Figure 3.5.10 illustrates the importance of aspect. In each of these diagrams, the lowest values of ENDVI are within BFLs and BHs, and the higher values are within the Moss class. Moss can experience low values of ENDVI, however, when facing the north or west, Moss typically has an increased ENDVI value.

3.4 DISCUSSION

3.4.1 *LAI and Aboveground Biomass*

Previous research has shown that ericaceous plants, such as *R. groenlandicum*, become more abundant immediately after fire in comparison to pre-fire conditions (Foster, 1985; Nguyen-Xuan *et al.*, 2000; Lecomte *et al.*, 2005). Strilesky and Humphreys (2011) found that in a *Sphagnum* and *Picea mariana* dominated peatland complexes, the aboveground biomass of *R. groenlandicum* was 75.6 g m^{-2} in an open bog and 100.8 g m^{-2} in a treed bog. The post-fire *R. groenlandicum* cover studied here showed that the aboveground biomass was 2.4 times that of the treed bog in EP-B and 3.0 times the treed bog in CP-B. The aboveground biomass for *R. groenlandicum* in CP-B and EP-B is 41% leaf mass. As the leaf longevity of *R. groenlandicum* is two years (Small, 1972), this 41% of the mass will continue to take in and store more carbon as leaves die and become leaf litter, even after these plants reach their maximum cover within each site.

LAI estimation has previously been conducted using many VIs, but the NDVI has been the most widely used VI in this estimation (Steltzer and Welker, 2006; Jones and Vaughan, 2010). However, Wang *et al.* (2007) found that by using green and blue reflectances in replacement of the red band in the NDVI to create a GBNDVI, a better estimation of LAI could be made. The data presented here shows that the best relationship between LAI and a VI is with the ENDVI, which utilizes green and blue reflectances as well. By using the relationship between ENDVI and *R. groenlandicum* LAI, it is possible to monitor the leaf cover and from that, estimations of the carbon intake of a peatland post-fire by this ericaceous species can also be made.

The aboveground biomass, dominated by *R. groenlandicum*, was higher within CP-B in comparison to EP-B. These ericaceous shrubs, which have deeply buried reproductive organs, have an ecological advantage after the passage of a low severity fire, colonizing burned bogs first (Flinn and Wein, 1977). When a high severity fire passes and the depth of burn (DOB) is high, these deeply buried reproductive organs are also burned resulting in the return of fewer plants immediately after fire (Lecomte *et al.*, 2005; 2006). Hokanson *et al.* (2015) found that the average DOB in CP-B (171-CPE) is 0.19 m and in EP-B (16-OEP) is 0.51 m. By applying the connection provided by Lecomte *et al.* (2005), that with a higher burn severity, the post-fire ericaceous shrub cover will be lower, the LAI and aboveground biomass data presented here matches the work conducted by Hokanson *et al.* (2015). By applying the relationship between ENDVI and *R.*

groenlandicum LAI, it is likely that the relative depth of burn between sites can be estimated using remote sensing.

Ericaceous shrubs can have a detrimental effect on tree regrowth due to their ability to influence ecosystem processes such as nutrient cycling (Nilsson *et al.*, 1993; Mallik and Mallik, 1997; Lecomte *et al.*, 2005). Although CP-B has had more aboveground biomass growth from ericaceous shrubs since the fire, it is likely that it will take longer for trees, such as *P. mariana*, to recolonize this site. As trees have denser biomass storage in comparison to shrubs, the establishment of *P. mariana* on EP-B will eventually result in this site having greater aboveground biomass than CP-B.

3.4.2 *Supervised Classification and Vegetation Indices*

The classification scheme applied to the ground layer had a substantial agreement (Landis and Koch, 1977) with the vegetation survey data. This particular classification would itself be classed as a no context, non-parametric, per pixel image-classification technique (Lu and Weng, 2007). While determining the class in which each individual pixel should be grouped, this classification scheme makes no assumptions about the structure of the data, treating every pixel as an individual, basing the class solely on its own spectral properties and not taking into account neighbouring pixels. This point classifier is one of the more commonly used styles of classifiers (Jones and Vaughan, 2010).

Lukenbach *et al.* (2015a) conducted a field study, which broadly classifies the ground percent cover within both EP-B and CP-B. The largest difference between the classification scheme presented here and the one presented by Lukenbach *et al.* (2015a) was between the percent cover of BFLs within EP-B. This discrepancy in the classification schemes was most likely caused by the plot size within EP-B, which only takes a 50 m^2 area into account, in comparison to Lukenbach *et al.* (2015a), who used a more broad approach across much of the peatland (0.5 ha).

The band distributions, which were the main factors in creating the classification scheme, only show slight variations among them, and as such, these differences by themselves are most likely not large enough to allow for the use of change detection in monitoring the recovery of a post-fire peatland. By using change detection algorithms or techniques, the pattern and extent of fire effects can be quantified (Miller and Yool, 2002). The use of VIs, in particular the change detection of the NDVI, has become increasingly more popular in burn severity mapping (Diaz-Delgado and Pons, 2001; Gitas *et al.*, 2009). However, using satellite-derived NDVI has been shown to be problematic in monitoring peatlands due to the lack of distinction between moss and higher vascular plants (Yuan *et al.*, 2013). The data presented here shows little separation in the NDVI and the GNDVI not only between the vascular overstory and the moss, but also between the BHs and the BFLs. The large distinctions between these classes provided by

the ENDVI suggests that it is the best suited VI for using change detection techniques to monitor not only burned peatlands, but peatlands in general.

As previous work has shown that after a fire, the distribution of vascular vegetation is independent of the groundcover distribution, the groundcover can be properly identified and then extrapolated for areas that are covered by overstory vegetation. This allows for a better understanding and representation of the ecosystem, allowing for more thorough post-fire monitoring. However, this particular technique is limited to lower remote sensing platforms as larger platforms (e.g. Thematic Mapper) have a lower resolution, allowing for the occurrence of the mixed pixel problem (Jones and Vaughan, 2010).

Lukenbach *et al.* (2015a) found that their classification scheme could be linked to landscape-scale properties and as such, they found a rapid and effective means for understanding the recovery within a *Sphagnum* dominated peatland post-fire. With the connection between the classification scheme presented by Lukenbach *et al.* (2015a) and the one presented here, it is likely that this classification scheme using remote sensing could also be linked to landscape-scale properties. This could provide a better and even faster means of understanding the recovery and trajectory post-fire of *Sphagnum* dominated peatlands.

Benscoter and Vitt (2008) found that the first 10 years post-fire were characterized by the dominance of true mosses. The colonization of these true mosses (e.g. *Polytrichum*) then facilitates the colonization of *Sphagnum*

(Benscoter, 2006). Three years post-fire, the colonization of these true moss species is clearly visible within both sites, and it is likely that both EP-B and CP-B will most likely be dominated by these species within the next several years. With the inclusion of these true moss patches within the Moss Layer of the classification scheme, their dominance in the first 10 years can be monitored, however, it is currently unknown how the spectral signature of a post-fire peatland will change as the peatland moves from true moss to *Sphagnum* dominance. By combining the classification scheme along with the change detection potential provided by ENDVI, the recovery of peatlands post-fire can be monitored with high accuracy and much more efficiency than ground truthing or surveying through the use of vegetation plots.

3.4.3 *Elevation and Aspect*

After three years post-fire, most of the lightly burned *S. fuscum* located on hummock tops within EP-B and CP-B has begun to recover. Within the BHs, *Ceratodon purpureus* and *Polytrichum* mosses have started recolonizing, supporting the findings of Benscoter (2006). Specifically, Benscoter (2006) found that within two years post-fire, a significant amount of ground layer colonization can occur, and that the majority of this colonization will take place in lower plots. Lukenbach *et al.* (2015a) found that the areas with the deepest burning exhibited the highest moisture contents post-fire. With colonization occurring in these BHs and *S. fuscum* recovery occurring on top of the hummocks,

it is very likely that the intermediate microtopographic areas will be the last to become re-vegetated (Benscoter and Vitt, 2008) as the vegetation will slowly encroach on these areas. Dominated by BFLs, the sides of these intermediate microtopographic areas exhibit low surface moisture and high tension (Lukenbach *et al.*, 2015a), which are unfavourable conditions for moss recolonization.

Pleurozium schreberi has a slight preference of growing facing the south on the side of hummocks in these intermediate microtopographic areas. Post-fire, these areas that have undergone light burning, stay dry, due to their hydrophobic properties (Kettridge *et al.*, 2014) and also from their orientation towards the sun, which furthers the inability for moss to recolonize. The highest ENDVI values (indicating the least amount of stress) generally occur on microtopographic areas orientated towards the north (Figure 3.5.9). This is very apparent within Figure 3.5.9b, where all high ENDVI values are either atop of hummocks or orientated towards the north, in areas that are dominated by *S. fuscum* recovery.

3.4.4 *Change Detection*

By using the remote sensing classification scheme presented here, remote sensing (i.e. using a UAV platform) can be utilized to allow for the use of change detection techniques to monitor plant response to fire. The subtraction of images (Diaz-Delgado and Pons, 2001) has previously been used to apply a VI to act as a surrogate for monitoring the chronosequence of vegetation recovery (Epting and Verbyla, 2005). With such a large difference in average values for the ENDVI

between the living plants (Moss and Vascular Layers) and the areas that have yet to recover (BFL and BH Layers), future research may show that by broadly applying the ENDVI to an entire peatland, it may be possible to monitor the vegetation trajectory of a post-fire peatland. This furthers previous work, by bringing in a spatial component to this recovery trajectory.

3.5 FIGURES

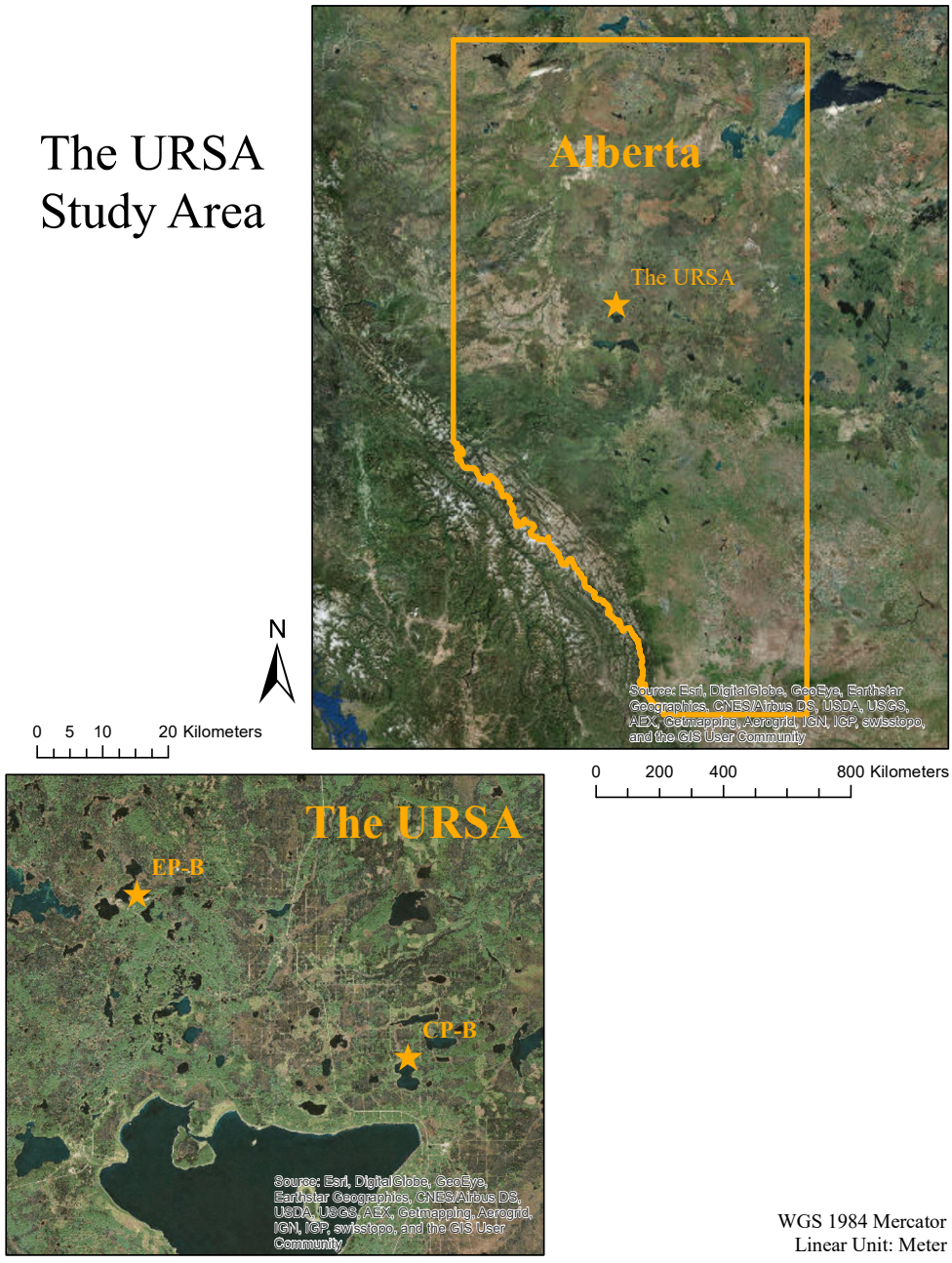

Figure 3.5.1: Map of the URSA

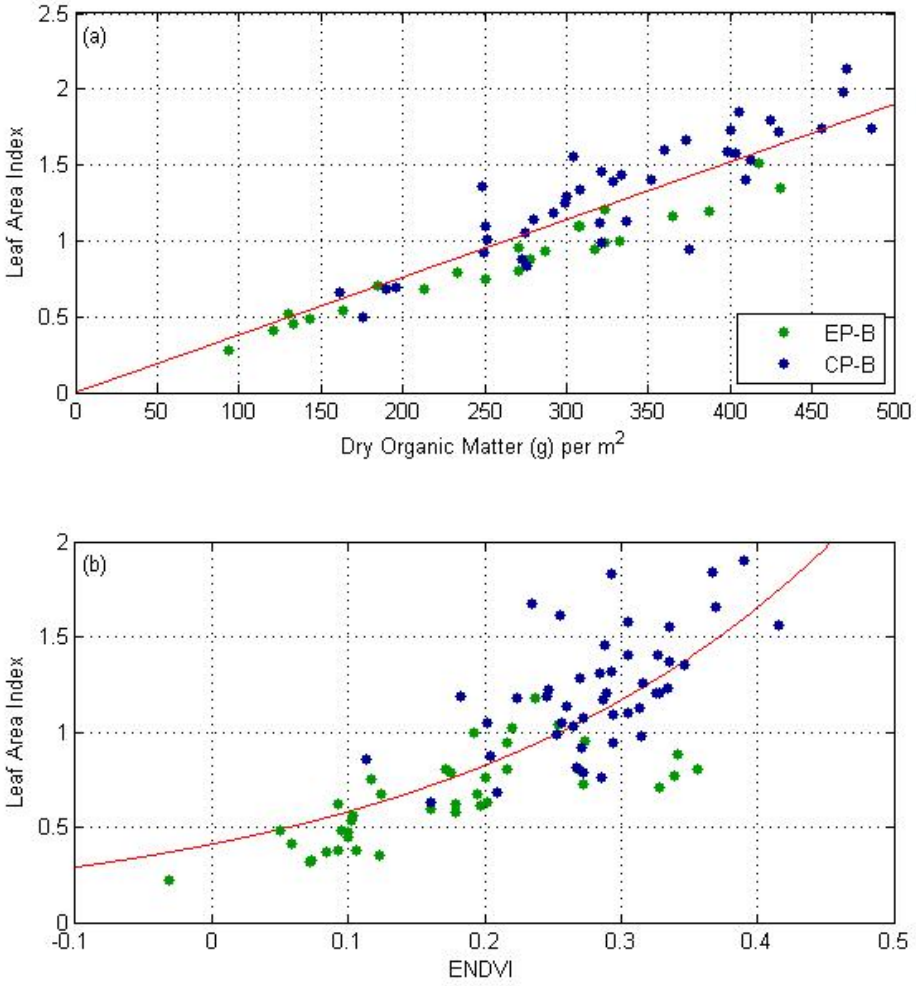

Figure 3.5.2: Leaf Area Index for both CP-B and EP-B plotted against (a) the dry organic matter ($R^2 = 0.814$, $p < 0.001$), and (b) the ENDVI ($R^2 = 0.687$, $p < 0.001$).

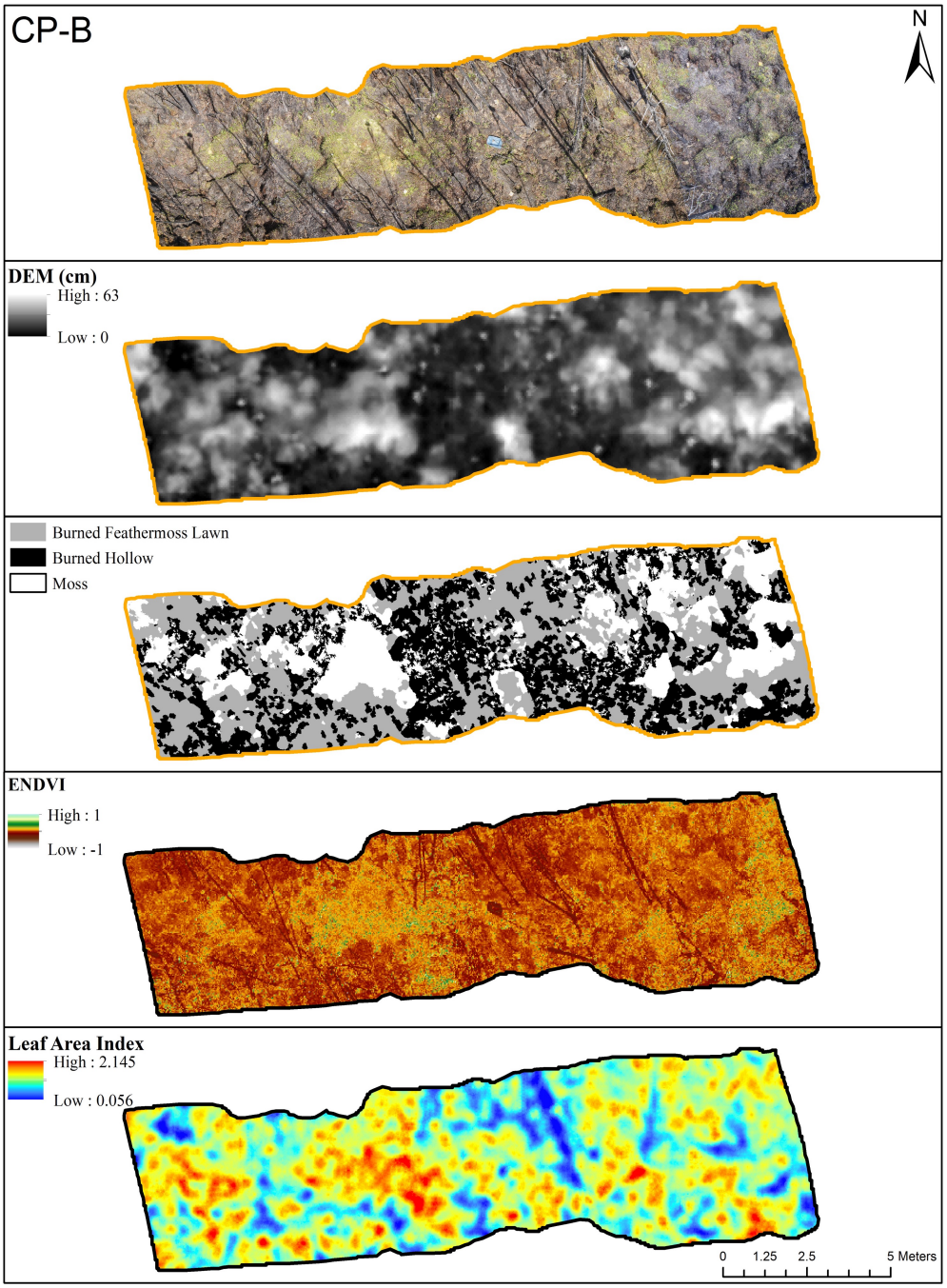

Figure 3.5.3: Plot within CP-B measuring roughly 5 m x 20 m. Top to bottom: RGB composite after removal of vascular vegetation, digital elevation model, ground layer classification, ENDVI of the ground layer, and Leaf Area Index distribution.

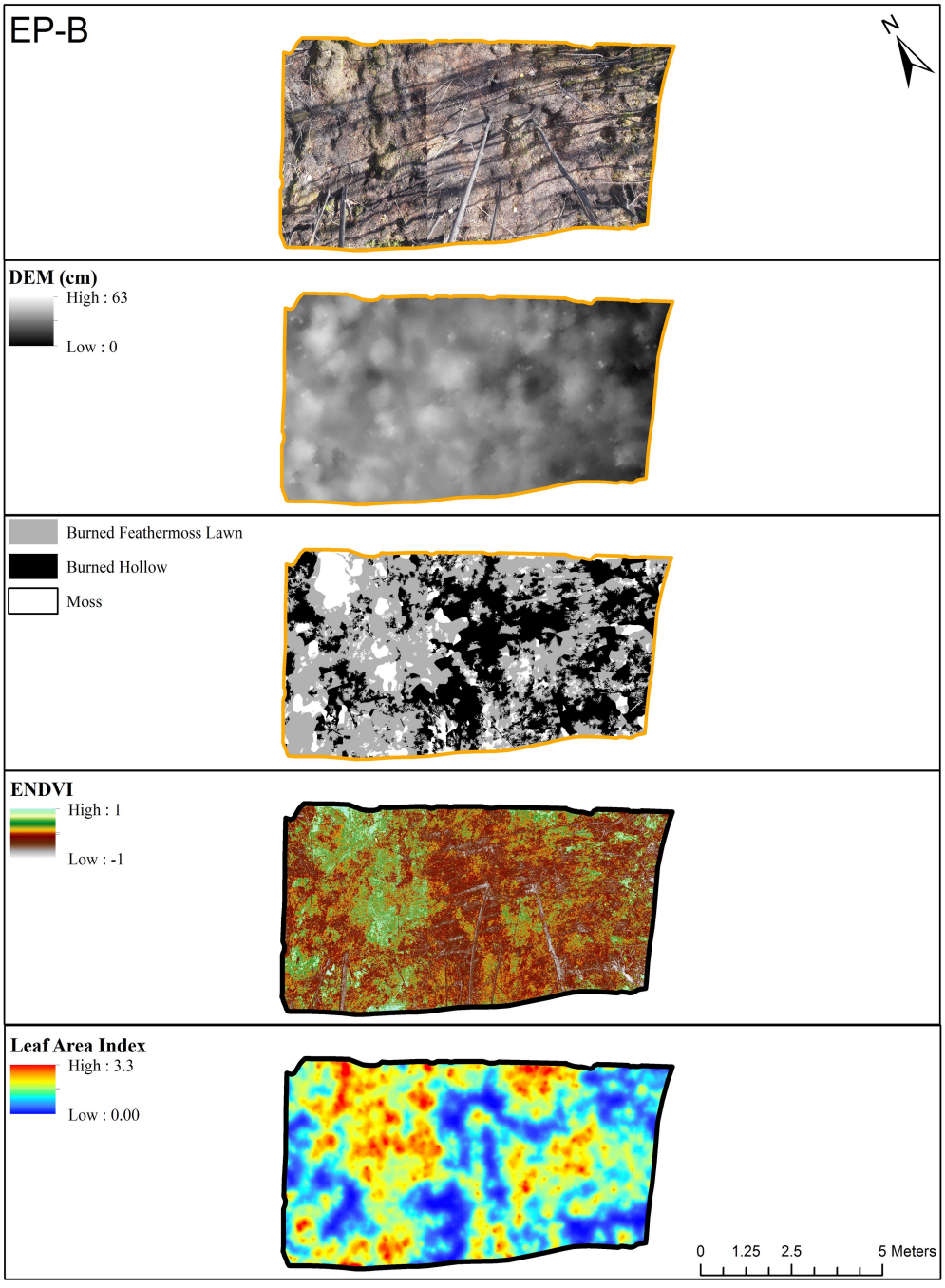

Figure 3.5.4: Plot within EP-B measuring roughly 5 m x 10 m. Top to bottom: RGB composite after removal of vascular vegetation, digital elevation model, ground layer classification, ENDVI of the ground layer, and Leaf Area Index distribution.

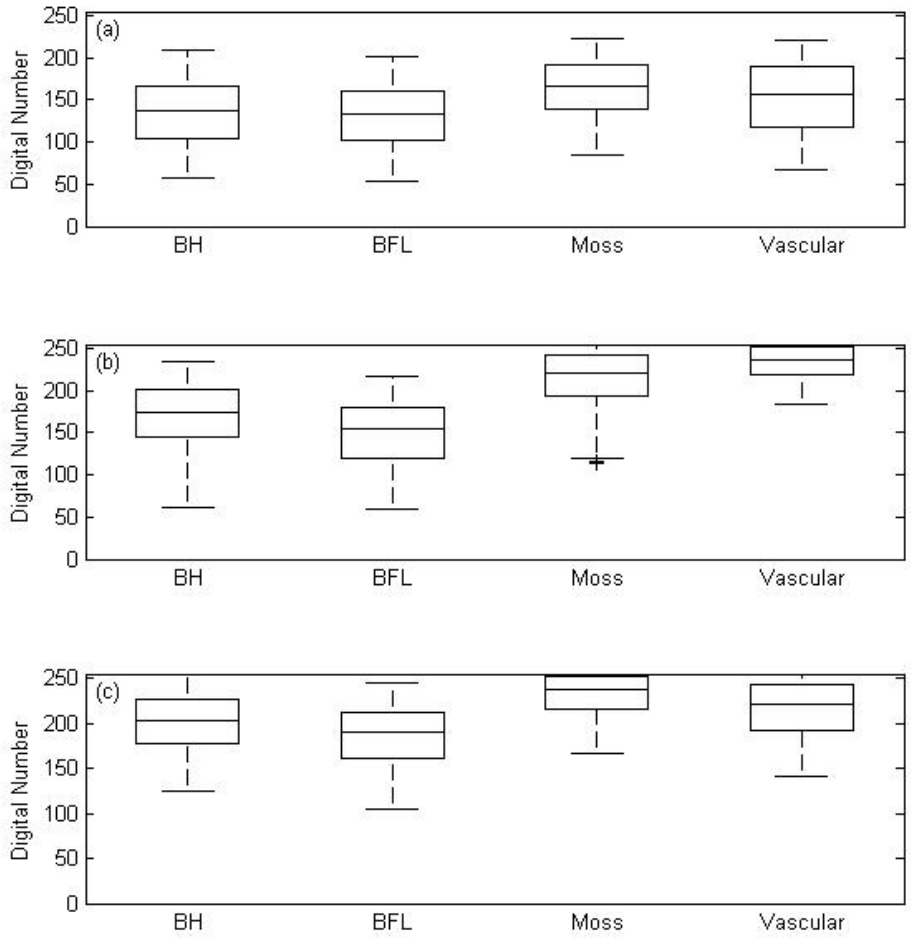

Figure 3.5.5: Distribution for the (a) red band, (b) NIR band, (c) UV-A band for the classification scheme within CP-B.

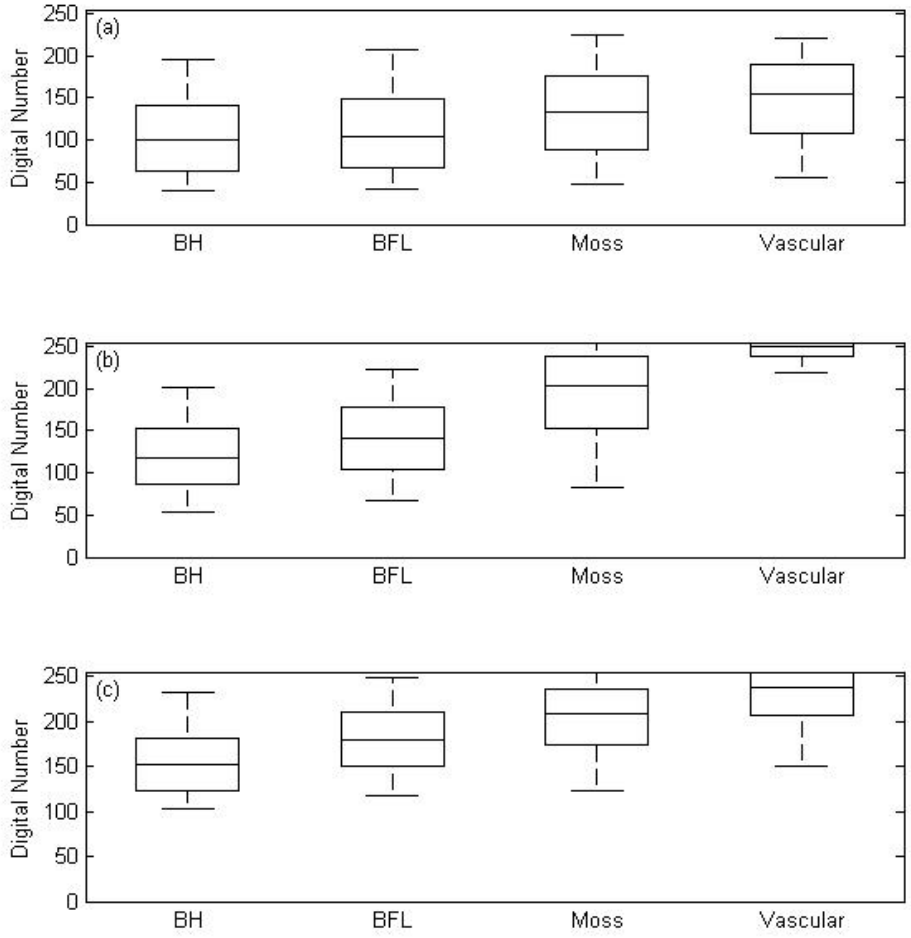

Figure 3.5.6: Distribution for the (a) red band, (b) NIR band, (c) UV-A band for the classification scheme within EP-B.

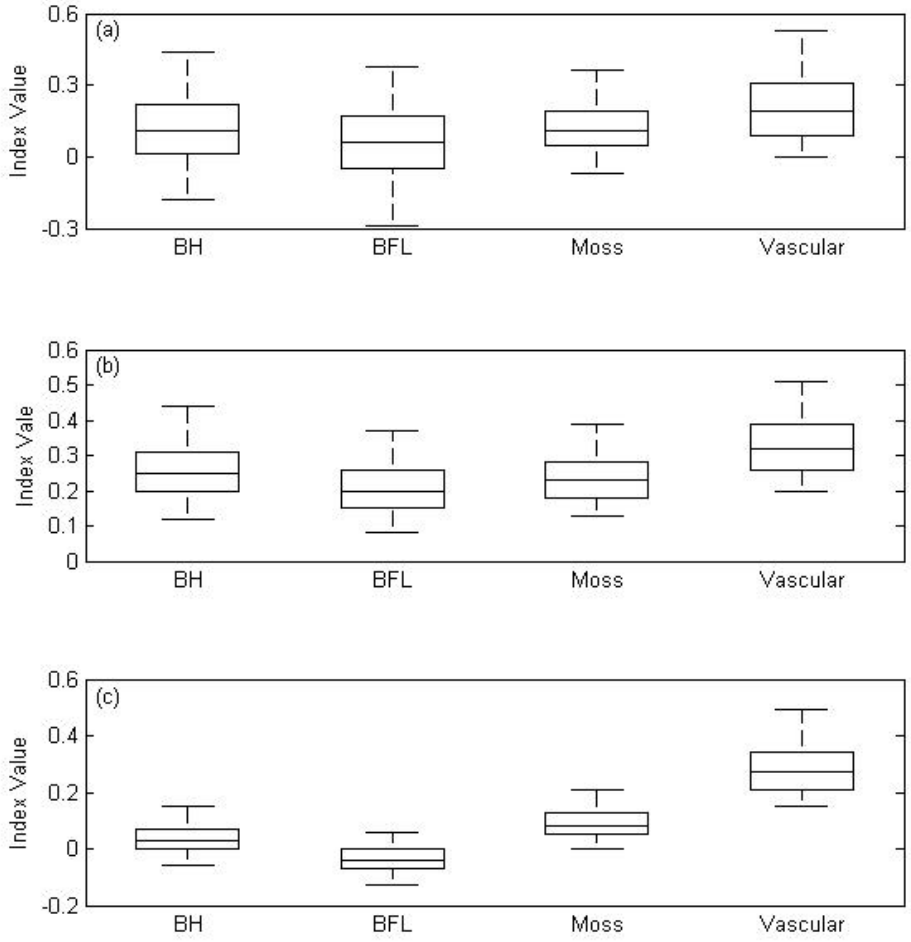

Figure 3.5.7: Distribution for the (a) NDVI, (b) GNDVI, (c) ENDVI for each of the classes within CP-B.

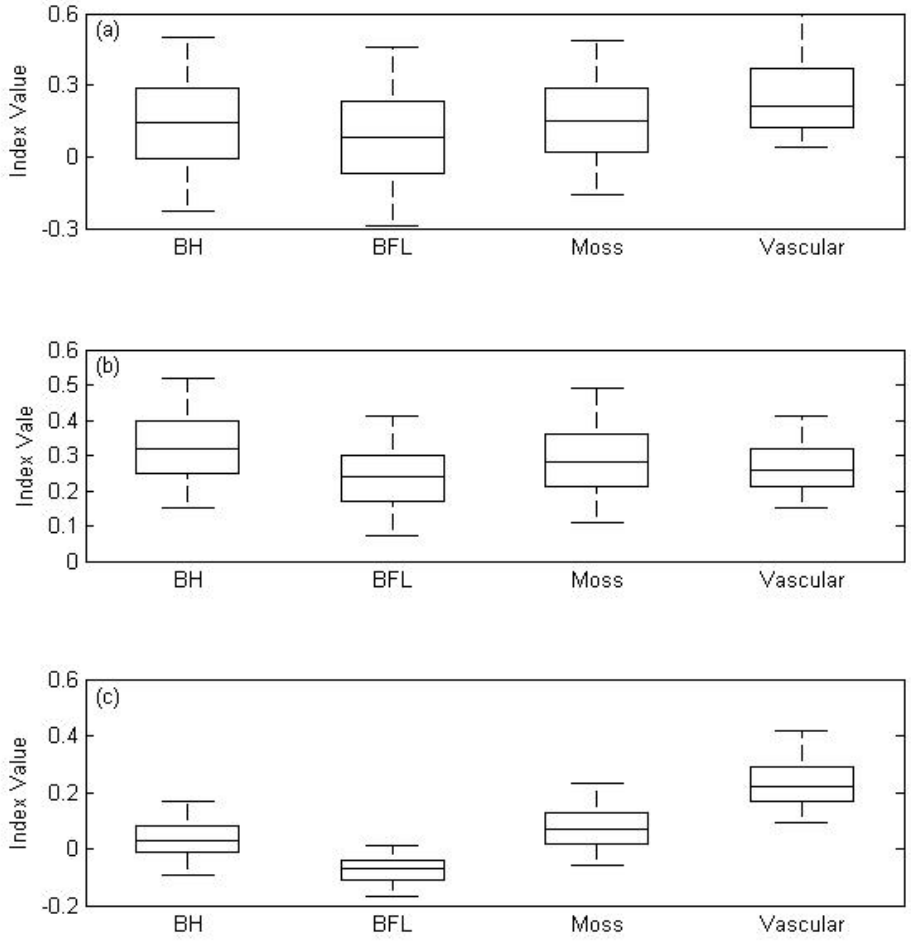

Figure 3.5.8: Distribution for the (a) NDVI, (b) GNDVI, (c) ENDVI for each of the classes within EP-B.

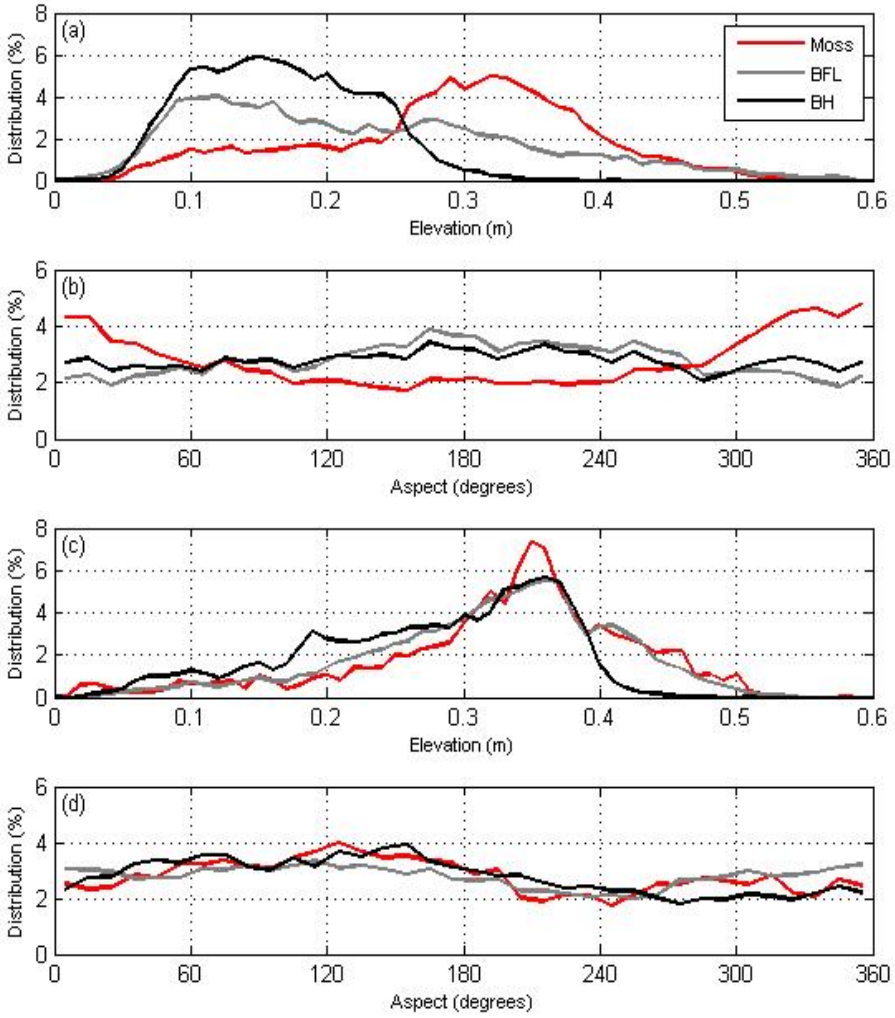

Figure 3.5.9: Distributions for the ground classification layers for elevation in (a) CP-B and (c) EP-B, as well as the distributions for the class' aspects in (b) CP-B and (d) EP-B.

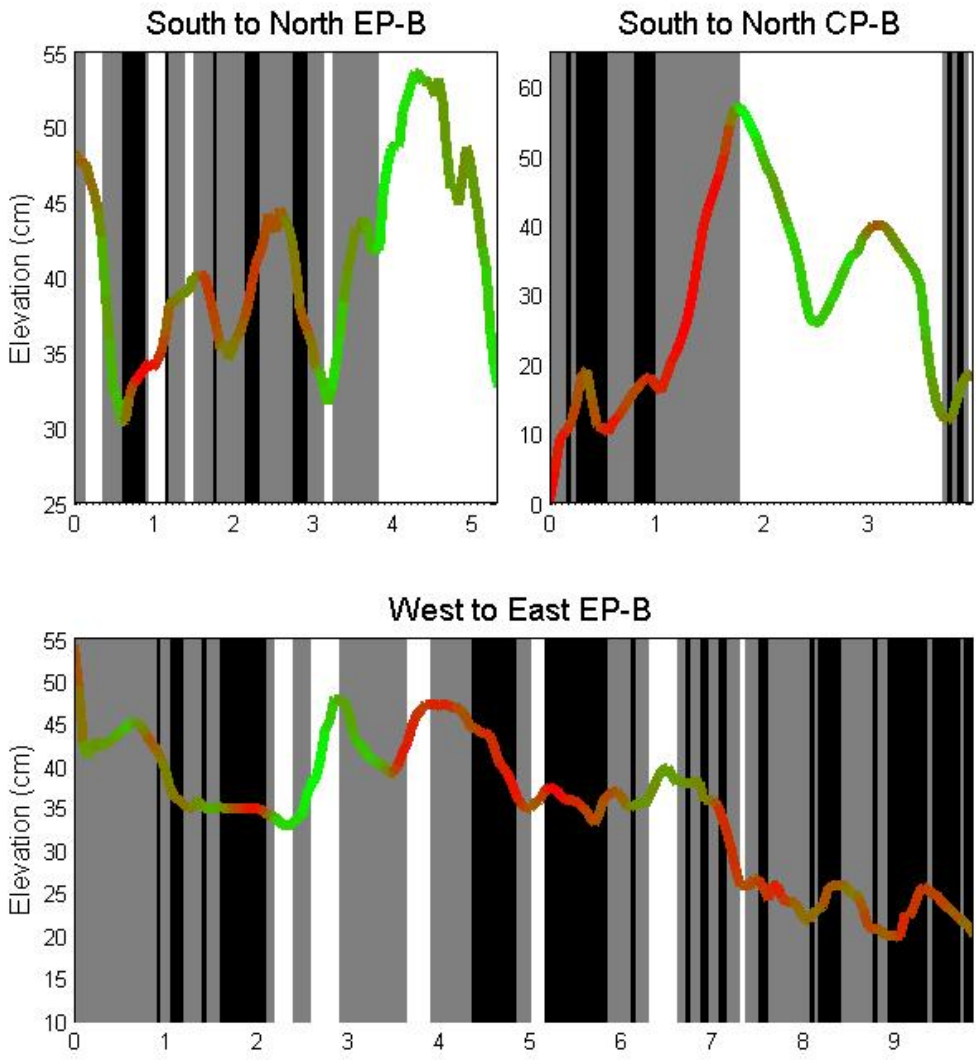

Figure 3.5.10: Elevation profiles showing the change in relative height on top of the distribution of the ground layer classification scheme, where white is Moss, gray is BFL, and black is BH. The colour of the line indicates that particular locations ENDVI value, where the brightest red is the lowest ENDVI value and bright green is the highest ENDVI value for that particular profile.

Table 3.5.11: Error matrix for the remote sensing classification scheme of CP-B

	Moss	**BFL**	**BH**	**Total**
Moss	436	18	59	513
BFL	22	118	22	162
BH	97	72	419	588
Total	555	208	500	**1263**

Overall Accuracy = 77.0%
$\hat{\mathbf{K}}$ = 0.627

Producer's Accuracy:
Moss = 78.6%
BFL = 56.7%
BH = 83.8%

User's Accuracy:
Moss = 84.9%
BFL = 72.8%
BH = 71.2%

Table 3.5.12: Error matrix for the remote sensing classification scheme of EP-B

	Moss	**BFL**	**BH**	**Total**
Moss	32	23	9	64
BFL	3	189	10	202
BH	5	51	309	365
Total	40	263	328	**631**

Overall Accuracy = 84.0%
$\hat{\mathbf{K}}$ = 0.714

Producer's Accuracy:
Moss = 80.0%
BFL = 71.8%
BH = 94.2%

User's Accuracy:
Moss = 50.0%
BFL = 93.6%
BH = 84.6%

CHAPTER 4: CONCLUSION

This research, in part, assessed the effectiveness of using thermal imaging and various vegetation indices to monitor peatlands, and more specifically *Sphagnum* moss 'health'. With *Sphagnum* moss productivity being strongly dependent on the near-surface moisture conditions and the proximity to the water table, it was expected that plots characterized with a higher surface temperature, would also have a low moisture content and *Sphagnum* productivity would also be low. Thermal imaging was compared to chlorophyll florescence, a measure of productivity to assess this relationship. Results from this study indicate that a threshold difference exists between *Sphagnum* productivity and surface temperature. When *Sphagnum* surface temperature exceeds a threshold value, *Sphagnum* quickly changes from being productive, to being unproductive.

Although the NDVI is the most widely used VI, it is not the best suited VI to monitor *Sphagnum*, as *Sphagnum* is not always green in colour. By utilizing the effectiveness of the NIR, green, and blue wavelengths to monitor chlorophyll activity, this research concluded that the ENDVI is best suited to monitor the 'health' of *Sphagnum* moss as a whole. The ENDVI, like the thermal imaging, shows a threshold difference as well. Specifically, where the ENDVI is high, the *Sphagnum* will be productive, and otherwise, the *Sphagnum* will be stressed. By utilizing both thermal imaging and the ENDVI to monitor peatlands and more specifically *Sphagnum* moss, it may be possible to decipher if unproductive

Sphagnum is water stressed, or if there is some other cause for it being unproductive. Moreover, these research findings have important carbon exchange modelling implications. It is possible that by quantifying this threshold response for various species, moss could potentially be modelled as a binary process (productive and unproductive).

This research also developed a classification scheme to aid in monitoring peatland recovery to fire disturbance, and to examine whether or not remote-sensing techniques could be applied to quickly and easily monitor a peatland on a larger scale. This brings a spatial component into monitoring the recovery of peatlands from wildfire. By utilizing the ENDVI, the vascular plant cover within a burned peatland can be mapped, allowing for a quick and easy method to monitoring LAI and aboveground biomass. Using the classification scheme presented here, the ground cover can be identified, which showed large differences in average values of ENDVI within each classification layer. By using these differences in average values, it may be possible to use the ENDVI value to monitor percent ground cover and with that, over time, use change detection techniques to monitor the change in ground cover. The remote sensing techniques outlined here for post-fire recovery of a peatland can not only be used to monitor the recovery trajectory of a peatland, but can potentially be applied to a peatland that has undergone other disturbances to aid in reclamation efforts and monitoring.

These findings highlight the potential uses of remote sensing to expansively and quickly aid peatland recovery monitoring, and assess the driving factors of *Sphagnum* moss stress. This work shows that the use of remote sensing platforms such as drones, can be utilized to monitor peatlands.

CHAPTER 5: REFERENCES

Bauer I.E., Gignac L.D., and Vitt D.H. 2003. Development of a peatland complex in boreal western Canada: lateral site expansion and local variability in vegetation succession and long-term peat accumulation. *Canadian Journal of Botany* **81**: 833-847.

Benscoter B.W. 2006. Post-fire bryophyte establishment in a continental bog. *Journal of Vegetation Science* **17**(5): 647-652.

Benscoter B.W., and Vitt D.H. 2008. Spatial patterns and temporal trajectories of the bog ground layer along a post-fire chronosequence. *Ecosystems* **11**(7): 1054-1064.

Benscoter B.W., and Wieder R.K. 2003. Variability in organic matter lost by combustion in a boreal bog during the 2001 Chisholm fire. Canadian Journal of Forest Research 33: 2509-2513.

Bilger W., Schreiber U., and Bock M. 1995. Determination of the quantum efficiency of photosystem II and of non-photochemical quenching of chlorophyll fluorescence in the field. *Oecologia* **102**(4): 425-432.

Bothe R.A., and Abraham C. 1993. Evaporation and evapotranspiration in Alberta 1986-1992 addendum. Surface Water Assessment Branch, Technical Services & Monitoring Division, Water Resources Services, Alberta Environmental Protection.

Bubier J.L., Rock B.N., and Crill P.M. 1997. Spectral reflectance measurements of boreal wetland and forest mosses. *Journal of Geophysical Research* **102**(24): 29,483-29,494.

Carter G.A. 1993. Responses of leaf spectral reflectance to plant stress. *American Journal of Botany* **80**(3): 239-243.

Chaerle L., and Van Der Straeten D. 2000. Imaging techniques and the early detection of plant stress. *Trends in Plant Science* **5**(11): 495-501.

Chapelle E.W., Kim M.S., and McMurtney III J.E. 1992. Ratio analysis of reflectance spectra (RARS): an algorithm for the remote estimation of the concentrations of chlorophyll a, chlorophyll b, and carotenoids in Soybean leaves. *Remote Sensing of the Environment* **39**: 239-247.

Clymo R.S., and Hayward P.M. 1982. The ecology of *Sphagnum*. In A.J.E.Smith (Ed.), *Bryophyte Ecology* (229-289). London, England: Chapman and Hall, 1982.

Congalton R.G, and Green K. 2009. *Assessing the Accuracy of Remotely Sensed Data: Principles and Practices* (2nd ed.). Boca Raton, FL: CRC Press.

Coppin P., Jonckheere I., Nackaerts K., Muys B., and Lambin E. 2004. Digital change detection methods in ecosystem monitoring: a review. *International Journal of Remote Sensing* **25**(9): 1565-1596.

Culshaw N., Corrigan D., Ketchum J., Wallace P., Wodicka N., and Easton R. 2004. Georgian Bay geological synthesis, Grenville Province: explanatory notes for preliminary maps p.3548 to p.3552. Ontario Geological Survey; Open File Report 6143, 28p.

Demmig B., and Björkman O. 1987. Comparison of the effect of excessive light on chlorophyll fluorescence (77K) and photon yield of O_2 evolution in leaves of higher plants. *Planta* **171**: 171-184.

Devito K.J., Mendoza C., and Qualizza C. 2012. *Conceptualizing water movement in the Boreal Plains. Implications for watershed reconstruction*. Synthesis report prepared for the Canadian Oil Sands Network for Research and Development, Environmental and Reclamation Research Group, 164p.

Diaz-Delgado R., and Pons X. 2001. Spatial patterns of forest fires in Catalonia (NE of Spain) along the period 1975-1995 analysis of vegetation recovery after fire. *Forest Ecology and Management* **147**: 67-74.

Dise N.B., Gorham E., and Verry E.S. (1993). Environmental factors controlling methane emissions from peatlands in northern Minnesota. *Journal of Geophysical Research* **98**: 10,583-10,594.

Epting J., and Verbyla D. (2005). Landscape-level interactions of pre-fire vegetation, burn severity, and postfire vegetation overa 16-year period in interior Alaska. *Canadian Journal of Forest Research* **35**: 1367-1377.

Faulkenham S.E., Hall R.I., Dillon P.J., and Karst-Riddoch T. (2003). Effects of drought-induced acidification on diatom communities in acid-sensitive Ontario lakes. *Limnology and Oceanography* **48**(4): 1662-1673.

Ferone J.M., and Devito K.J. (2004). Shallow groundwater-surface water interactions in pond-peatland complexes along a Boreal Plains topographic gradient. *Journal of Hydrology* **292**(4): 75-95.

Flinn M.A., and Wein R.W. (1977). Depth of underground plant organs and theoretical survival during fire. *Canadian Journal of Botany* **55**: 2550-2554.

Foster D.R. (1985). Vegetaion development following fire in *Picea mariana* (black spruce)-*Pleurozium* forests of south-eastern Labrador, Canada. *Journal of Ecology* **73**: 517-534.

Freeman C., Lock M.A., and Reynolds B. (1993). Fluxes of CO_2, CH_4, and N_2O from a Welsh peatland following simulation of water table draw-down: potential feedback to climatic change. *Biogeochemistry* **19**: 51-60.

Gerdol R., Bonora A., Gualandri R., and Pancaldi S. (1996). CO_2 exchange, photosynthetic pigment composition, and cell ultrastructure of *Sphagnum* mosses during dehydration and subsequent rehydration. *Canadian Journal of Botany* **74**: 726-734.

Gerdol, R., and Vicentini R. (2011). Response to heat stress of populations of two Sphagnum species from alpine bogs at different altitudes. *Environmental and Experimental Botany* **74**: 22-30.

Gitas I.Z, de Santis A., and Mitri G.H. 2009. Remote sensing of burn severity. In E. Chuvieco (Ed.), *Earth Observation of Wildland Fires in Mediterranean Ecosystems* (129-148). Berlin, Germany: Springer.

Gitelson A.A., and Merzlyak M.N. (1998). Remote sensing of chlorophyll concentration in higher plant leaves. *Advances in Space Resources* **22**(5): 689-692.

Gitelson A.A., Gritz Y., and Merzlyak M.N. (2003). Relationships between leaf chlorophyll content and spectral reflectance and algorithms for non-destructive chlorophyll assessment in higher plant leaves. *Journal of Plant Physiology* **160**: 271-282.

Gitelson A.A., Kaufman Y.J., and Merzlyak M.N. (1996). Use of a green channel in remote sensing of global vegetation from EOS-MODIS. *Remote Sensing of the Environment* **58**: 289-298.

González-Rodríguez G., Colubi A., and Gil M.A. (2012). Fuzzy data treated as functional data: A one-way ANOVA test approach. *Computational Statistics and Data Analysis* **56**: 943-955.

Gorham E. (1991). Northern peatlands: role in the carbon cycle and probable responses to climatic warming. *Ecological Applications* **1**(2): 182-195.

Gorham J. (1990). Phenolic compounds, other than flavonoids, from bryophytes. In Zinsmeister H.D., and Mues R. (Eds.), *Bryophytes. Their Chemistry and Chemical Taxonomy* (171-200). Oxford, England: Claredon Press.

Gouveia C.M., Bastos A., Trigo R.M., and DaCamara C.C. (2012). Drought impacts on vegetation in the pre-and post-fire events over Iberian Peninsula. *Natural Hazards and Earth System Sciences* **12**: 3123-3137.

Granath G., Moore P.A., Lukenbach M.C., Waddington J.M. (2016). Mitigating wildfire carbon loss in managed northern peatlands through restoration. *Scientific Reports* **6**(28498): 9pp.

Grosvernier P., Matthey Y., and Buttler A. (1997). Growth potential of three *Sphagnum* species in relation to water table level and peat properties with implications for their restoration in cut- over bogs. *Journal of Applied Ecology* **34**(2): 471-483.

Harris A. (2008). Spectral reflectance and photosynthetic properties of Sphagnum mosses exposed to progressive drought. *Ecohydrology* **1**: 35-42.

Harris A., Bryant R.G., and Baird A.J. (2005). Detecting near-surface moisture stress in *Sphagnum* spp. *Remote Sensing of Environment* **97**: 371-381.

Heiberger R.M., and Holland B. (2006). Mean-mean multiple comparison displays for families of linear contrasts. *Journal of Computational and Graphical Statistics* **15**(4): 937-955.

Hokanson K.J., Lukenbach M.C., Devito, K.J., Kettridge N., Petrone R.M., and Waddington J.M. (2015). Groundwater connectivity controls peat burn severity in the boreal plains. *Ecohydrology* **9**(4): 574-584.

Huete A.R., Liu H.Q., Batchily K., and van Leeuwen W. (1997). A comparison of vegetation indices over a global set of TM images for EOS-MODIS. *Remote Sensing of Environment* **59**: 440-451.

Hunt Jr. E.R., Doraiswamy P.C., McMurtrey J.E., Daughtry C.S.T., Perry E.M., and Akhmedov B. (2013). A visible band index for remote sensing leaf chlorophyll content at the canopy scale. *International Journal of Applied Earth Observation and Geoinformation* **21**: 103-112.

Ingram H.A.P. (1982). Size and shape in raised mire ecosystems: a geophysical model. *Nature* **297**: 300-303.

Intergovernmental Panel on Climate Change (IPCC). 2007. Solomon S. et al. (Eds.), *Climate Change 2007: The Scientific Basis. Contribution of Working Group I to the Fourth Assessment Report of the Intergovernmental Panel on Climate Change*. New York, NY: Cambridge Univ. Press.

Jin S. (2014). Accuracy assessment for classification and modeling. In Wang G., and Weng Q. (Eds.), *Remote Sensing of Natural Resources* 45-56. Boca Raton, FL: CRC Press.

Johnson M.G., Granath G., Tahvanainen T., Pouliot R., Stenøien H.K., Rochefort L., *et al.* (2015). Evolution of niche preference in Sphagnum peat mosses. *Evolution* **69**(1): 90-103.

Jones H.G., and Vaughan R.A. (2010). Remote sensing of vegetation: principles, techniques, and applications. New York, NY: Oxford University Press.

Kalaji H.M., Govindjee, Bosa K., Kościelniak J., and Żuk-Golaszewska K. (2011). Effects of salt stress on photosystem II efficiency and CO_2 assimilation of two Syrian barley landraces. *Environmental and Experimental Botany* **73**: 64-72.

Kasischke E.S., French N.H.F., Harrell P., Christensen Jr. N.L., Ustin S.L., and Barry D. (1993). Monitoring of wildfires in Boreal forests using large area AVHRR NDVI composite image data. *Remote Sensing of Environment* **45**: 61-71.

Kellner E. (2001). Surface energy fluxes and control of evapotranspiration from a Swedish Sphagnum mire. *Agricultural and Forest Meteorology* **110**: 101-123.

Kettridge N., Thompson D.K., and Waddington J.M. (2012). Impact of wildfire on the thermal behavior of northern peatlands: observations and model simulations. *Journal of Geophysical Research: Biogeosciences* 117 (G2).

Kettridge N., and Waddington J.M. (2014). Towards quantifying the negative feedback regulation of peatland evaporation to drought. *Hydrological Processes* **28**: 3728-3740.

Kettridge N., Humphrey R.E., Smith J.E., Lukenbach M.C., Devito K.J., Petrone R.M., and Waddington J.M. (2014). Burned and unburned peat repellency: implications for peatland evaporation following wildfire. *Journal of Hydrology* **513**: 335-341.

Kolenosky G.B., and Johnston D.H. (1967). Radio-tracking Timber Wolves in Ontario. *American Zoologist* **7**: 289-303.

Landis J.R., and Koch G.G. (1977). The measurement of observer agreement for categorical data. *Biometrics* **33**: 159-174.

Lecomte N., Simard M., and Bergeron Y., Larouche A., Asnong H., and Richard P.J.H. (2005). Effects of fire severity and initial tree composition on understorey vegetation dynamics in a boreal landscape inferred from chronosequence and paleoecological data. *Journal of Vegetation Science* **16**: 665-674.

Lecomte, N., Simard M., and Bergeron Y. (2006). Effects of fire severity and initial tree composition on stand structural development in the coniferous boreal forest of northwestern Québec, Canada. *Ecoscience* **13**(2): 152-163.

Letendre J., Poulin M., and Rochefort L. (2008). Sensitivity of spectral indices to CO2 fluxes for several plant communities in a *Sphagnum*-dominated peatland. *Canadian Journal of Remote Sensing* **34**(2): 414-425.

Lichtenthaler H.K., and Babani F. (2000). Detection of photosynthetic activity and water stress by imaging the red chlorophyll fluorescence. *Plant Physiology and Biochemistry* **38**(11): 889-895.

Lichtenthaler H.K., and Miehé J.A. Fluorescence imaging as a diagnostic tool for plant stress. *Trends in Plant Science* **2**(8): 316-320.

Lu D., and Weng Q. (2007). A survey of image classification methods and techniques for improving classification performance. *International Journal of Remote Sensing* **28**(5): 823-870.

Lu D., Mausel P., Brondízio E., and Moran E. (2004). Change detection techniques. *International Journal of Remote Sensing* **25**(12): 2365-2407.

Lukenbach M.C., Devito K.J., Kettridge N., Petrone R.M., and Waddington J.M. (2015a). Hydrogeological controls on post-fire moss recovery in peatlands. *Journal of Hydrology* **530**: 405-418.

Lukenbach M.C., Devito K.J., Kettridge N., Petrone R.M., and Waddington J.M. (2015b). Burn severity alters peatland moss water availability: implications for post-fire recovery. *Ecohydrology* **9**(2): 341-353.

Lutes D.C., Keane R.E., Caratti J.F., Key C.H., Benson N.C., Sutherland S., *et al*. (2006). FIREMON: Fire effects monitoring and inventory system gen. tech. rep. RMRS-GTR-164-CD. Fort Collins, CO: US Department of Agriculture Forest Service.

Lunetta R. S., Knight J.F., Ediriwickrema J., Lyon J.G., and Worthy L.D. (2006). Land-cover change detection using multi-temporal MODIS NDVI. *Remote Sensing of Environment* **105**: 142-154.

Mallik I., and Mallik A.U. (1997). Effects of *Ledum groenlandicum* amendments on soil characteristics and black spruce seedling growth. *Plant Ecology* **133**(1): 29-36.

Marshall Jr. J.C., Manning J.V., and Kingsbury B.A. (2006). Movement and macrohabitat selection of the Eastern Massasauga in a fen habitat. *Herpetologica* **62**(2): 141-150.

Miller J.D., and Yool S.R. (2002). Mapping forest post-fire canopy consumption in several overstory using multi-temporal Landsat TM and ETM data. *Remote Sensing of Environment* **82**: 481-496.

Murray K.J., Tenhunen J.D., and Nowak R.S. (1993). Photoinhibition as a control on photosynthesis and production of *Sphagnum* mosses. *Oecologia* **96**: 200-207.

Nguyen-Xuan T., Bergeron Y., Simard D., Fyles J.W., and Paré D. (2000). The importance of forest floor disturbance in the early regeneration patterns of the boreal forest of western and central Quebec: a wildfire versus logging comparison. *Canadian Journal of Forest Research* **30**: 1353-1364.

Nichols D.S., and Brown J.M. (1980). Evaporation from a *Sphagnum* moss surface. *Journal of Hydrology* **48**: 289-302.

Nilsson M.C., Högberg P., Zackrisson O., and Fengyou W. (1993). Allelopathic effects by *Empetrum hermaphroditum* on development and nitrogen uptake by roots and mycorrhizae of *Pinus silvestris*. *Canadian Journal of Botany* **71**: 620-628.

Padilla F.M., Peña-Fleitas M.T., Gallardo M., Thompson R.B. (2014). Evaluation of optical sensor measurements of canopy reflectance and of leaf flavonols and chlorophyll contents to assess crop nitrogen status of muskmelon. *European Journal of Agronomy* **58**: 39-52.

Proctor M.C.F., and Smirnoff N. (2000). Rapid recovery of photosystems on rewetting desiccation-tolerant mosses: chlorophyll fluorescence and inhibitor experiments. *Journal of Experimental Botany* **51**(351): 1695-1704.

Providenti M.A., Lee H., and Trevors J.T. (1993). Selected factors limiting the microbial degradation of recalcitrant compounds. *Journal of Industrial Microbiology* **12**: 379-395.

Rascher U., Liebig M., and Lüttge U. (2000). Evaluation of instant light-response curves of chlorophyll fluorescence parameters obtained with a portable chlorophyll fluorometer on site in the field. *Plant, Cell and Environment* **23**: 197-1405.

Robichaud P., Lewis S.A., Laes D.Y.M., Hudak A.T., and Kokaly R.F. (2007). Postfire soil burn severity mapping with hyperspectral image unmixing. *Remote Sensing of Environment* **108**: 467-480.

Rochefort L. (2000). *Sphagnum* – A keystone genus in habitat restoration. *The Bryologist* **103**(3): 503-508.

Roulet N., Moore T., Bubier J., Lafleur P. (1992). Northern fens: methane flux and climatic change. *Tellus B* **44**(2): 100-105.

Rudolph H., and Jöhnk A. (1982). Physiological aspects of phenolic compounds in the cell walls of *Sphagna*. *The Journal of the Hattori Botanical Laboratory* **53**: 195-203.

Ruxton G.D. (2006). The unequal variance *t*-test is an underused alternative to Student's *t*-test and the Mann-Whitney *U* test. *Behavioral Ecology* **17**(4): 688-690.

Shetler G., Turetsky M.R., Kane E., and Kasischke E. (2008). Sphagnum mosses limit total carbon consumption during fire in Alaskan black spruce forests. *Canadian Journal of Forest Research* **38**: 2328-2336.

Singh A. (1989). Digital change detection techniques using remotely-sensed data. *International Journal of Remote Sensing* **10**(6): 99-1003.

Small E. (1972). Photosynthetic rates in relation to nitrogen recycling as an adaptation to nutrient deficiency in peat bog plants. *Canadian Journal of Botany* **50**: 2227-2233.

Smerdon B.D., Mendoza C.A., and Devito K.J. (2012). The impact of gravel extraction on groundwater dependent wetlands and lakes in the Boreal Plains, Canada. *Environmental Earth Sciences* **67**(5): 1249-1259.

Steltzer H., and Welker J.M. (2006). Modeling the effect of photosynthetic vegetation properties on the NDVI-LAI relationship. *Ecology* **87**(11): 2765-2772.

Stoline M.R. (1981). The status of multiple comparisons: simultaneous estimation of all pairwise comparisons in one-way ANOVA designs. *The American Statistician* **35**(3): 134-141.

Strilesky S.L., and Humphreys E.R. (2012). A comparison of the net ecosystem exchange of carbon dioxide and evapotranspiration for treed and open portions of a temperate peatland. *Agricultural and Forest Meteorology* **153**: 45-53.

Tarnocai C. (2006). The effect of climate change on carbon in Canadian peatlands. *Global and Planetary Change* **53**: 222-232.

Thiele A., and Krause H. (1994). Xanthophyll cycle and thermal energy dissipation in photosystem II: relationship between zeaxanthin formation, energy-dependent fluorescence quenching and photoinhibition. *Journal of Plant Physiology* **144**(3): 324-332.

Thompson D.K., and Waddington J.M. (2008). *Sphagnum* under pressure: towards an ecohydrological approach to examining *Sphagnum* productivity. *Ecohydrology* **1**: 299-308.

Titus J.E., Wagner D.J., and Stephens M.D. (1983). Contrasting water relations of photosynthesis for two *Sphagnum* mosses. *Ecology* **64**(5): 1109-1115.

Tuker C. J. (1979). Red and photographic infrared linear combinations for monitoring vegetation. *Remote Sensing of Environment* **8**: 127-150.

Tuittila E., Vasander H., and Laine J. (2004). Sensitivity of C sequestration in reintroduced *Sphagnum* to water-level variation in a cutaway peatland. *Restoration Ecology* **12**(4): 483-493.

Turetsky M., Wieder K., Halsey L., and Vitt D. (2002). Current disturbance and the diminishing peatland carbon sink. *Geophysical Research Letters* **29**(11): 1526-1528.

van Breeman N. (1995). How *Sphagnum* bogs down other plants. *Trends in Ecology and Evolution* **10**(7): 270-275.

Van Gaalen K.E., Flanagan L.B., and Peddle D.R. (2007). Photosynthesis, chlorophyll fluorescence and spectral reflectance in *Sphagnum* moss at varying water contents. *Oecologia* **153**: 19-28.

van Kooten O., and Snel J.F.H. (1990). The use of chlorophyll fluorescence nomenclature in plant stress physiology. *Photosynthesis Research* **25**: 147-150.

Vitt D.H. (1990). Growth and production dynamics of boreal mosses over climatic, chemical and topographic gradients. *Botanical Journal of the Linnean Society* **104**: 35-59.

Vogelmann J.E., and Moss D.M. (1993). Spectral reflectance measurements in the genus *Sphagnum*. *Remote Sensing of Environment* **45**: 273-279.

Waddington J.M., Morris P.J., Ketttridge N., Granath G., Thompson D.K., and Moore P.A. (2015). Hydrological feedbacks in northern peatlands. *Ecohydrology* **8**: 113-127.

Wang F., Huang J., Tang Y., and Wang X. (2007). New vegetation index and its application in estimating Leaf Area Index of Rice. *Rice Science* **14**(3): 195-203.

Wieder W.R., Cleveland C.C., Townsend A.R. (2009). Controls over leaf litter decomposition in wet tropical forests. *Ecology* **90**(12): 3333-3341.

Williams T.G., and Flanagan L.B. (1996). Effect of changes in water content on photosynthesis, transpiration and discrimination against $^{13}CO_2$ and $C^{18}O^{16}O$ in *Pleurozium* and *Sphagnum*. *Oecologia* **108**: 38-46.

Yoder B.J., and Waring R.H. (1994). The Normalised Difference Vegetation Index of small Douglas-fir canopies with varying chlorophyll concentrations. *Remote Sensing of Environment* **49**: 81-91.

Yuan W., Liu S., Dong W., Liang S., Zhao S., Chen J., et al. (2013). Differentiating moss from higher plants is critical in studying the carbon cycle of the boreal biome. *Nature Communications* **5**.

Zarco-Tejada P.J., Miller J.R., Mohammed G.H., Noland T.L., and Sampson P.H. (2002). Vegetation stress detection through chlorophyll a + b estimation and fluorescence effects on hyperspectral imagery. *Journal of Environmental Quality* **31**(5): 1433-1441.

Zoltai S.C., Morrissey L.A., Livingston G.P., and de Groot W.J. (1998). Effects of fires on carbon cycling in North American boreal peatlands. *Environmental Reviews* **6**(1): 13-24.